CHALMERS
UNIVERSITY OF TECHNOLOGY

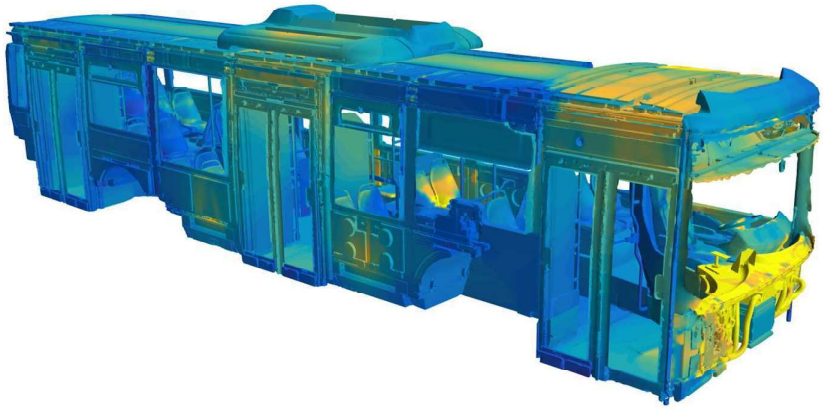

Modelling of Heat Transfer through Bus Body

Master's thesis in Applied Mechanics

Udhaya Bhaskhar Kumar
Shisheer Shetty

DEPARTMENT OF MECHANICS AND MARITIME SCIENCES

CHALMERS UNIVERSITY OF TECHNOLOGY
Gothenburg, Sweden 2023
www.chalmers.se

MASTER'S THESIS IN APPLIED MECHANICS

Modelling of heat transfer through bus body

SHISHEER SHETTY
UDHAYA BHASKHAR KUMAR

Department of Mechanics and Maritime Sciences
Division of Fluid Dynamics
CHALMERS UNIVERSITY OF TECHNOLOGY

Göteborg, Sweden 2023

Modelling of heat transfer through bus body
SHISHEER SHETTY
UDHAYA BHASKHAR KUMAR

Department of Mechanics and Maritime Sciences
Division of Fluid Dynamics
Chalmers University of Technology
SE-412 96 Göteborg
Sweden
Telephone: +46 (0)31-772 1000

Cover:
Image shows surface temperature of the bus body without any transparent surfaces

Chalmers Reproservice
Göteborg, Sweden 2023

Modelling of heat transfer through bus body
Master's thesis in Applied Mechanics
SHISHEER SHETTY
UDHAYA BHASKHAR KUMAR
Department of Mechanics and Maritime Sciences
Division of Fluid Dynamics
Chalmers University of Technology

Abstract

Electric buses are catching up and form a major part of the public transport system in major cities. The sustainability and low environmental impact of these buses make them a good option for use in major cities. However, efficiency is a key factor that makes them an attractive option. The HVAC system in these buses, responsible for making rides comfortable, is one of the largest energy consumers. It is essential to study the flow of heat in the bus to optimize the usage of these systems. A realistic simulation that accounts for all types of heat transfer could provide a much higher level of accuracy and give us valuable insight.

In this Master Thesis, a method was developed for simulating the interior climate and the heat transfer that happens through the bus's body. The methodology used a pseudo-transient model with a co-simulation of STAR-CCM+ and TAITherm. Multiple CFD steady-state simulations are run on STAR-CCM+ to account for the convection part of the heat transfer. Steady-state and transient simulations run in TAITherm simulate the conduction and radiation in the bus. These two models are coupled at multiple instances to simulate the transient physics while reducing the heavy computational times involved in transient CFD simulations. This approach has advantages and shortcomings, as will be discussed further in this thesis. The model was tested for a weather condition of -5 °Celsius.

Keywords: Electric buses, heat transfer, co-simulation, CFD, HVAC

Preface

This thesis is a part of Masters in Applied Mechanics at Chalmers University of Technology. The work was carried out at Volvo Buses with the help of supervisor, Nithin Bharadwaj Ravindra and examiner at Chalmers, Prof. Lars Davidsson

Acknowledgements

We would like to express our deepest gratitude to our supervisor Nithin Bharadwaj Ravindra, for his constant support during the entire course of the thesis. His experience and insight ensured a very smooth sailing through all the obstacles we faced. We would also like to thank Siemens for their support with all our doubts with the software. From TAITherm, we would like to thank Kameswara Kethireddy and Vishnuvardhan Ranganathan for their support with the software and also with developing the methodology. Lastly, we would like to thank Prof. Lars Davidson from Chalmers University of Technology for giving us support and guidance throughout the master's programme and for being our examiner.

Abbrevations

CFD - Computational fluid dynamics
HTC - Heat Transfer Coefficient
SGR - Surface Growth Rate
h - convective heat transfer coefficient
Tfluid - Temperature of fluid
Eq. - Equation
Eqs. - Equations
Fig. - Figure
FMT - Field Mean Temperature
mins - minutes

Nomenclature

t = Time
T = Temperature
μ = Dynamic viscosity
ρ = Density
v_i = Velocity in i-direction
x_i = Location in i-direction
σ_{ij} = Stress tensor
τ_{ij} = Viscous stress tensor
f_i = Body forces
P = Pressure
δ_{ij} = Identity tensor
S_{ij} = Strain-rate tensor
z = Radiative heat source
k = Thermal conductivity
u = Internal energy
c_p = Specific heat capacity at constant pressure
$q_{conduction}$ = Conductive heat flux
$q_{convection}$ = Convective heat flux
$q_{radiation}$ = Radiative heat flux
h = Convective heat transfer coefficient
E_b = Emissive power of the black body
$_{tr}$ = Stefan-Boltzmann constant
F_{1-2} = View factor from surface 1 to surface 2

Contents

1 Introduction

1.1 Background

Electric Buses play an important role in public transportation in sustainable cities like Gothenburg. While these buses have many advantages over traditional buses, one of their major drawbacks is their range. Operating these buses at the highest efficiency possible is of great importance. Maintaining interior climate is one of the most energy-intensive processes in electric buses, significantly affecting the driving range. Extreme weather conditions require constant temperature regulation in the cabin to maintain passenger comfort. Improving the efficiency of this system can reduce energy consumption and provide the all-important gains required in the range.

Analyzing the heat transfer from the bus's interior to the surrounding environment is vital to finding the right balance between energy consumption and interior climate quality. Although experimental analysis is reliable, it is often expensive and requires much more time to set up and test for multiple relevant cases. A more viable option is developing a fast and robust simulation method to accurately model heat transfer. Also, it allows an option to study the impact of choosing different materials for the bus body on the interior climate system.

In this thesis, a thermal model is developed with a CFD and a thermal solver to accurately and robustly predict heat transfer through the bus body.

1.2 Objective

The thesis aims to fulfill the following goals:

- Study and analyze interior climate through the existing CFD steady state model in Siemens STAR-CCM+
- Reduce the number of mesh elements in the CFD model to improve the mapping of values and reduce solving times
- Distinguish parts from the original geometry to include the material layer properties in TAITherm
- Create a mesh for TAITherm to include the newly added parts using reduced CFD mesh as a template
- Build a thermal model in TAITherm that includes conduction and radiation
- Select and develop a methodology to couple STAR-CCM+ and TAITherm, which will include transient analysis of the thermal case
- Comparing the different parts to find the high heat loss parts.

1.3 Limitations

The following limitations apply to this thesis:

- The simulations were not verified with experimental data, and the methodology could not be validated due to time constraints
- Although radiation from the different parts of the bus was considered, solar radiation was not considered
- For the radiation calculation, patches were utilized to speed up the process, which trades accuracy to reduce the time required to calculate the view factors
- Parts not covered by internal surface wrappers were not considered, including the outer body, which will be exposed to the outside environment in real life due to the increased complexity.
- Some parts having air gaps greater than 12.7mm were assumed to be a part of the outer body and not considered in the TAITherm thermal model. The reason is that air gaps above 12.7mm fall outside the validation range of the empirical formulae used in TAITherm for simulating air gaps

- Thermal properties of materials were considered constant irrespective of temperature.
- Conventional automotive glass property was utilized instead of the custom glass properties obtained from different vendors to reduce complexity
- Assumptions were made for the parts with non-availability of parts data like thickness, number of layers and the material used.
- For the outside convection, the heat transfer coefficient value of air is assumed to simplify the simulation.

Most of these limitations could have been overcome with much tighter planning, more time availability and computational resources for TAITherm simulations. Additionally, learning new software like TAITherm and ANSA and researching articles to establish a methodology consumed a significant portion of the time.

1.4 Ethical considerations

The methodology developed for the thesis is robust. It allows for a detailed thermal model simulation of electric vehicles like buses and cars, so it would significantly contribute to UN sustainable development goals "Sustainable Cities and Communities" and "Climate Action" [10] by allowing iterative design improvements that contribute towards increasing the driving range and reducing the power consumption. Another objective of the thesis is to present our findings simply and comprehensively, facilitating easy replication and further research.

2 Theory

2.1 Governing equations

Equations of mass conservation, momentum conservation and energy conservation govern heat transfer and fluid flow simulations. These equations form the basis on which even the most complex simulations are carried out.

2.1.1 Continuity

Continuity, also known as the mass conservation equation, is given by [2]:

$$\frac{d\rho}{dt} + \rho\frac{\partial v_i}{\partial x_i} = 0 \tag{2.1}$$

For incompressible flow cases, as in this case, it is constant, so the equation becomes:

$$\frac{\partial v_i}{\partial x_i} = 0 \tag{2.2}$$

2.1.2 Momentum

The equations which govern the conservation of momentum are also called Navier-Stokes equations; these equations also facilitate the transport of momentum in any Newtonian viscous flows [2]. The linear momentum balance equation must be expanded to obtain the Navier-Stokes equations. The momentum balance equation states that the linear momentum acting on a fluid particle is equal to the sum of the forces acting on it, which is given by:

$$\rho\frac{dv_i}{dt} = \frac{\partial \sigma_{ji}}{\partial x_j} + \rho f_i \tag{2.3}$$

where,

$$\sigma_{ij} = -P\delta_{ij} + 2\mu S_{ij} - \frac{2}{3}\mu S_{kk}\delta_{ij} \tag{2.4}$$

$$\tau_{ij} = 2\mu S_{ij} - \frac{2}{3}\mu S_{kk}\delta_{ij} \tag{2.5}$$

Now substituting the above terms in the 2.3 equation, Navier-Stokes equations are obtained as defined below:

$$\rho\frac{du_i}{dt} = -\frac{\partial P}{\partial x_i} + \frac{\partial \tau_{ji}}{\partial x_j} + \rho f_i = -\frac{\partial P}{\partial x_i} + \frac{\partial}{\partial x_j}\Big(2\mu S_{ij} - \frac{2}{3}\mu\frac{\partial v_k}{\partial x_k}\delta_{ij}\Big) + \rho f_i \tag{2.6}$$

For incompressible flows because of continuity equation 2.2, the Navier-Stokes equation reduces to:

$$\rho\frac{du_i}{dt} = -\frac{\partial P}{\partial x_i} + \frac{\partial}{\partial x_j}\Big[\mu\Big(\frac{\partial u_i}{\partial x_j} + \frac{\partial u_j}{\partial x_i}\Big)\Big] + \rho f_i \tag{2.7}$$

2.1.3 Energy

According to the first law of thermodynamics, the change in internal energy equals the heat transfer into the system and the net work done on the system [7].

From [3], the equation for energy conservation with radiation source included is:

$$\rho\frac{du}{dt} = \sigma_{ji}\frac{\partial v_i}{\partial x_j} - \frac{\partial q_i}{\partial x_i} + \rho z \tag{2.8}$$

Now from Fourier's law, the heat flux vector is:

$$q_i = -k\frac{\partial T}{\partial x_i} \tag{2.9}$$

Using Eqs. 2.4 and 2.5 in Eq. 2.8 we get:

$$\rho\frac{du}{dt} = -P\frac{\partial v_i}{\partial x_i} + \underbrace{2\mu\dot{S}_{ij}S_{ij} - \frac{2}{3}\mu S_{kk}S_{ii}}_{\Phi} + \frac{\partial}{\partial x_i}\left(k\frac{\partial T}{\partial x_i}\right) + \rho z \tag{2.10}$$

where $S_{ij}\partial v_i/\partial x_j = S_{ij}\left(S_{ij} + \Omega_{ij}\right)$, now since the product of a symmetric tensor, S_{ij}, and an anti-symmetric tensor, Ω_{ij}, is zero, the $S_{ij}\left(S_{ij} + \Omega_{ij}\right)$ becomes equal to $S_{ij}S_{ij}$.

For an incompressible flow,

$$du = c_p dT \tag{2.11}$$

$$-P\frac{\partial v_i}{\partial x_i} = 0 \tag{2.12}$$

Assuming c_p to be constant and using Eqs. 2.11 and 2.12 in Eq. 2.10, the energy balance equation is [2]:

$$\rho c_p\frac{dT}{dt} = \Phi + \frac{\partial}{\partial x_i}\left(k\frac{\partial T}{\partial x_i}\right) + \rho z \tag{2.13}$$

Here, Φ is the dissipation term. The term represents irreversible viscous heating which is negligible for incompressible flows [2]. The second and third terms in Eq. 2.13 represent heat flux due to conduction and radiation, respectively [4].

2.2 Heat transfer

Heat transfer is an essential focus of the thesis, so relevant theories are discussed here to acquaint the readers with the subject.

2.2.1 Conduction

The heat transfer that occurs when two or more solid bodies come into contact is called conduction. Here, heat transfer occurs by kinetic energy transfer due to the collision of molecules. The conduction heat transfer can be expressed using Fourier's law in 1D form as:

$$q_{conduction} = -kA\frac{dT}{dx} \tag{2.14}$$

2.2.2 Convection

Convection is the heat transfer that occurs between a solid surface and fluid. According to Newton's law of cooling, the heat transfer rate can be expressed as:

$$q_{convection} = hAdT \tag{2.15}$$

Eq. 2.15 indicates that the heat transfer rate is proportional to the temperature difference between the solid body and the surrounding fluid environment.

There are two types of convection: forced and natural convection. For interior climate simulations of vehicles, especially in very cold environmental conditions, modelling accurate natural convection is paramount due to the significant buoyancy effect present caused by the differences in density [7].

2.2.3 Radiation

Radiation is a type of heat transfer where no medium is required. All bodies that have a temperature above absolute zero emit thermal radiation. Stefan-Boltzmann law gives the maximum emission from a black body, according to the law:

$$E_b = \sigma_{tr} T^4 \tag{2.16}$$

where,

σ_{tr} has a value of 5.670374 x $10^{-8} \frac{W}{m^2 K^4}$
T is the absolute temperature in K.

Multiplying area to Eq. 2.16 gives heat transfer rate,

$$q_{radiation} = A\sigma_{tr} T^4 \tag{2.17}$$

Now, the general radiation heat transfer equation that covers all the surfaces is:

$$q_{radiation} = \epsilon A\sigma_{tr} T^4 \tag{2.18}$$

where,

ϵ is 1 for a black body

When considering radiation heat transfer from one body to another, an additional term called view factor is needed. So the heat transfer equation becomes:

$$q_{radiation} = \epsilon A F_{1-2} \sigma_{tr} (T_1 - T_2)^4 \tag{2.19}$$

The view factor quantitatively measures radiative flux leaving from surface 1 that strikes surface 2. In simple terms, the view factor measures how well one surface can see another.

For a cold surface, the radiative heat transfer is lower than a hot surface, so at lower temperatures, the radiation mode of heat transfer becomes less significant [8].

2.2.4 Properties that affect the thermal behaviour of a material

Thermal conductivity

Thermal conductivity defines the ability of a material to conduct heat. If the thermal conductivity of a material is very low, the material acts as an insulator. High thermal conductive materials can be used in places that need cooling down/heating up, for example, fins. In Eq. 2.14, k is the thermal conductivity it is expressed with SI units $W/m.K$

Specific Heat Capacity

The specific heat is defined as the amount of heat required (J) to raise the temperature of a unit mass (1kg) of a material by 1 K. It has the SI units of $J/Kg.K$. A material with a high specific heat capacity will have a low heat transfer rate as more heat is required to raise the temperature of the material.

Density

The density of a material is an important factor to consider when carrying out transient heat transfer analysis. In Eq. 2.13, the right-hand side term is not zero for a transient case as the temperature changes with time. Material with higher density will have lower thermal diffusivity, i.e., as the density of material increases, heat conduction occurs much slower.

Emissivity

Emissivity is the ratio of the energy thermally radiated by the surface of a material to the energy radiated by a perfect emitter, also known as the blackbody. Emissivity is a dimensionless number represented by ϵ. For a blackbody, the value of emissivity is 1, whereas, for a perfect reflector, the value of emissivity is 0.

Irradiation

The total thermal radiation per unit area of a body receives is called irradiation. Denoted by G

Absorptivity

Absorptivity defines the ratio of the total irradiation reaching a surface that is absorbed. The absorbed radiation will heat the body. It is denoted by α_{tr}. The absorptivity of a black body is 1.

Reflectance

Reflectance is the ratio of total irradiation that is reflected by a body. It is denoted by ρ_{tr}. The reflectance of a pure reflector is 1.

Transmittance

Transmittance is the ratio of total irradiation that will transmit through a material. Transmittance is only applicable if a body is not opaque. It is described by τ_{tr}.

For any surface of a material,

$$\alpha_{tr} + \tau_{tr} + \rho_{tr} = 1 \tag{2.20}$$

2.2.5 Transparent material

Unlike opaque parts, where the absorptivity and reflectivity depend on the surface condition, transparent parts depend on the thickness of the part and the material property instead of a surface condition. In this case, the surface condition is only used for finding the thermal emissivity. Furthermore, in the transparent parts, transmittance will be taken into account. [11]

2.2.6 Air gaps

In TAITherm, air gap convection and radiation are found using an empirical formulation that only holds for air gap thicknesses less than 12.7mm. The heat transfer coefficient is given by:

$$hc = 21.8\frac{(1.0 + 0.00274T)}{L} \tag{2.21}$$

Here,

T is the mean temperature of the two plates in $°C$,
hc is the heat transfer coefficient in $W/m^2.K$ and,
L is the gap width in mm

2.3 Transient analysis and thermal diffusivity

The equation 2.9 represents heat conduction under steady-state conditions where ∇T is constant. When ∇T changes with time, the heat conduction is:

$$\rho c\frac{\partial T}{\partial t} = \frac{\partial}{\partial x_i}\left(k\frac{\partial T}{\partial x_i}\right) \tag{2.22}$$

Here, $k/(\rho c_p)$ is the thermal diffusivity usually represented as α. Thermal diffusivity is an essential parameter in transient analysis as it influences the thermal inertia of a material via the characteristic time scale. Thermal

inertia is the ability of a material to resist temperature changes. A material with high thermal inertia will heat up and cool down slower than one with lower thermal inertia. Thermal inertia is inversely proportional to thermal diffusivity, i.e., a material with high thermal diffusivity will have lower thermal inertia so that the material will have a faster response to temperature change.

2.4 Transient analysis and number of layers

The mass of a part is divided among the thermal nodes present in a part. In transient analysis, the thermal response of any particular node changes depending on the mass. So, the thermal gradient is more accurately captured when the number of layers increases. Therefore, increasing the number of layers increases the accuracy of the transient solution. The best practice is to keep increasing the number of nodes till the solution no longer changes [5]. Since increasing the number of layers increases the computational cost and complexity due to the different layers of materials present, the practice is not adopted for this thesis.

2.5 Planar and cylindrical conduction types

Using the planar conduction type, the order of the materials does not matter as long as there is no air gap. When an air gap is present, according to the materials' order, the surface conditions on both sides of the air gap change, affecting radiation results, whereas, in the cylindrical conduction type, the order of the materials used will affect the thermal results; having a highly conductive material inside the cylinder with low conductive materials outside will result in more heat transfer compared to the cylinder having less conductive material in the inner surface.

For simplicity, only the planar layer type is considered in the thesis for all the parts.

2.6 Turbulence model used

The turbulent flow in the bus cabin and the HVAC system is modelled using the Realizable Two-layer K-Epsilon turbulence model in our simulation. The k-ϵ model solves the transport equations for turbulent kinetic energy (k) and turbulent dissipation rate (ϵ), determining turbulent eddy viscosity. The turbulent viscosity is computed as [2],

$$\nu_t = c_\mu \frac{k^2}{\epsilon} \tag{2.23}$$

The Two-Layer approach allows the k-ϵ model to be applied in the viscous-affected layer. With this approach, in the layer next to the wall, the turbulent dissipation rate and turbulent viscosity are specified as functions of wall distance. The values specified in the near-wall region are blended with those computed from solving the transport equations away from the wall.[9]

Realizability means that the model meets the mathematical criteria on the Reynolds stresses, which are more consistent with the actual physics of turbulence in flows. The Realizable Two-Kayer K-Epsilon model combines a new formulation for the turbulent dissipation rate with the benefits of the two-layer approach described earlier.

2.7 Components of HVAC system present in the CFD model

The Heating, Ventilation, and Air Conditioning (HVAC) system of the bus maintains the interior climate of the cabin at a comfortable level for the passengers. The HVAC system takes care of the cabin's heating and cooling, depending on the ambient temperatures. Figure 2.1 shows the major components of the HVAC system, the Rooftop AC Unit, Convectors, Heat Blowers and Defroster.

Roof top AC unit

The rooftop AC unit has cooling and heating modes. When operated in cooling mode, it removes heat from the bus using evaporators. It is equipped with heat pumps, which makes it possible to operate them in heating mode. Both modes use the blowers for their operation [7].

Convectors

Convectors exchange heat from hot water to the surrounding air via natural convection; they have increased surface area to improve the heat transfer [7].

Heat Blowers

Heat Blowers are similar in functionality to Convectors but rely on force convection via blowers to exchange heat [7].

Defroster

The main functionalities of the defroster include defogging and cleaning the windshield and controlling the climate around the bus driver. For this purpose, it is equipped with a heat exchanger, evaporator, air filter and a blower [7].

Since the model from the previous work is used in this thesis, only the overview of the components is provided. For more details and the method adopted to model the HVAC components in CFD, please refer [7]

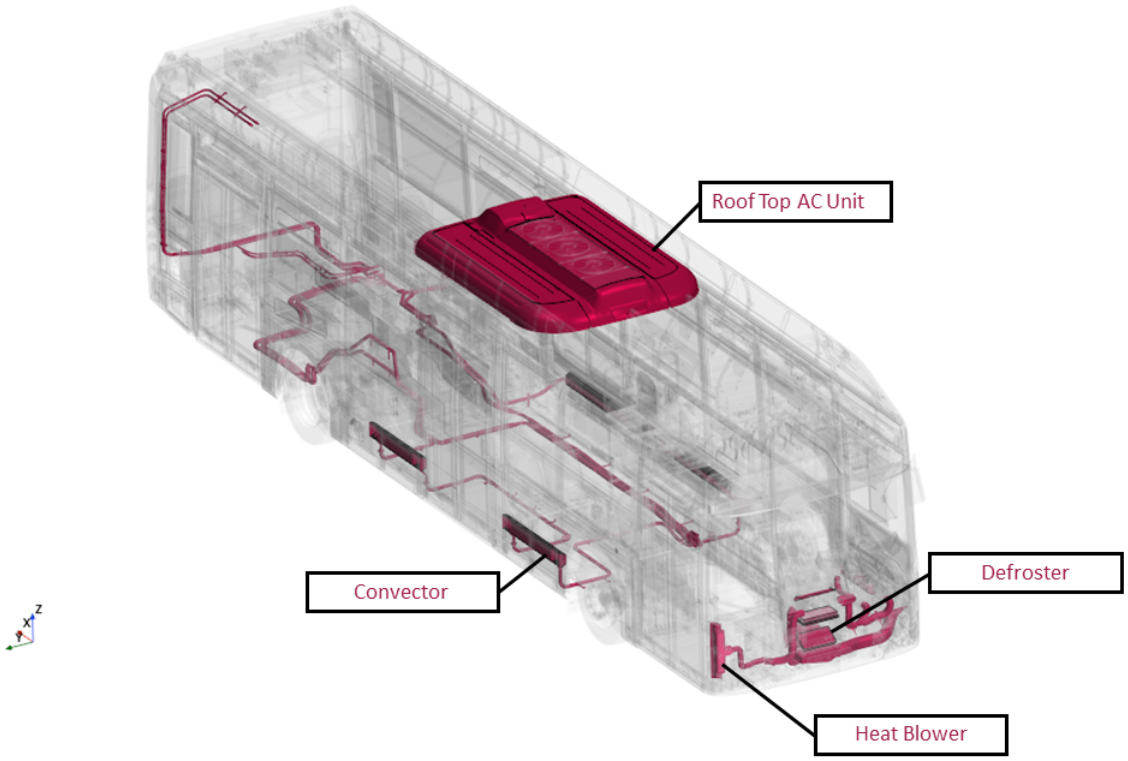

Figure 2.1: Components of HVAC System

3 Method

The process followed to set up the simulation of the interior climate of the bus and study the heat transfer through the bus body is described in this chapter. The method development was based on the earlier studies made for similar simulations.

The tools used during the simulation are ANSA for pre-processing and STAR-CCM+ for simulation of the CFD for the convection part of the heat transfer, and TAITherm for the conduction and radiation.

3.1 STAR-CCM+

3.1.1 Mesh

Surface Wrapper

The complex geometry of the bus can create issues when volume meshing. Hence, it is suggested to have a surface wrapper. The Surface Wrapper is a tool in STAR-CCM+ that creates a closed, manifold and non-intersecting surface mesh from the surface of the bus. The wrapper clears up the surface and covers all the small gaps in the geometry imported from ANSA.

A single surface wrapper is used with the gap closure function active. A mesh study was done to compare the settings for the surface wrap. The study aimed to have a mesh fine enough to capture the details of all the parts on the bus's interior while comparatively keeping the CFD model computationally light. The Surface Remesher tool is then used to refine and improve the quality of the surface mesh. Figures 3.1 and 3.12 show the bus before and after the surface wrap. As visible, the parts outside the volume of interest are not included in the surface wrap. Figures 3.3 and 3.4 show the inside of the bus.

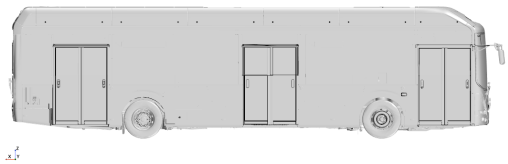

Figure 3.1: Actual Bus

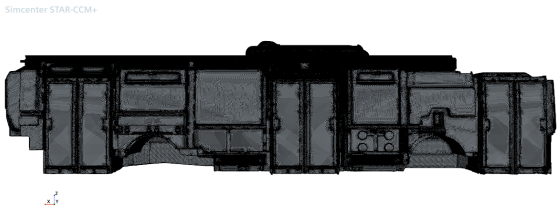

Figure 3.2: Surface Wrap

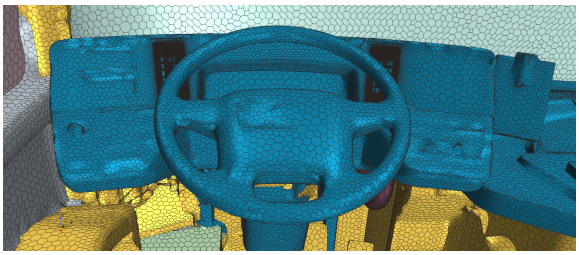

Figure 3.3: Surface Wrap of Dashboard

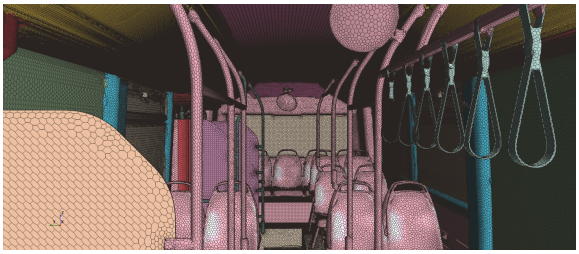

Figure 3.4: Surface Wrap of the Interior of the Bus

A study was carried out to compare different configurations of the surface mesh. The aim was to keep the model computationally light while also ensuring the bus's geometry was captured accurately. Due to the complexity of the geometry, and the wide range of sizes of parts involved, a normal single-size meshing strategy did not seem

possible. Custom controls were created according to the size of parts and the expected refinement required in certain regions. The created custom controls allowed the mesh to stay relatively light while achieving a relatively high level of fidelity with the geometry. According to the guidelines from Taitherm experts, keeping the CFD mesh on the coarser side was also necessary to enable more accurate coupling with Taitherm. Table 3.12 shows the Default settings that were used for the Surface Wrap, and table 3.2 show the parts that were excluded from the default settings and were meshed with different settings. Using multiple custom controls for most parts allowed the use of a much coarser wrap in regions of lower interest and bigger geometry.

Default Settings	
Base Size	100 mm
Target Surface Size	40 mm
Minimum Surface Size	15 mm
Surface Curvature	36
Gap Closure	Seed Points
Volume of Interest	Seed Points

Table 3.1: Default Surface Wrap Settings

Custom Controls		
Parts	**Target Surface Size**	**Minimum Surface Size**
AC	20 mm	5 mm
AC Cover	20 mm	5 mm
AC Heat Exchangers	4 mm	1 mm
AC Roof Blower	10 mm	5 mm
Air Duct	10 mm	5 mm
Bars	15 mm	10 mm
Base Parts	30 mm	15 mm
Convectors	5 mm	1 mm
Dashboard	25 mm	10 mm
Defroster	10 mm	5 mm
Defroster - Air Filter	5 mm	0.25 mm
Defroster - Airpipes	5 mm	1 mm
Defroster - Heat Exchangers	5 mm	1 mm
Defroster - Outlet Duct	10 mm	5 mm
Doors	30 mm	15 mm
Handles	15 mm	7 mm
Heaters	5 mm	1 mm
Inlet Holes	1 mm	0.5 mm
Mirror	30 mm	10 mm
Recirc	5 mm	1 mm
Seats	30 mm	15 mm
Shields	30 mm	15 mm

Table 3.2: Custom Controls used for Surface Wrap

Volume Mesh

The Volume Mesh for the bus was generated using the Automated Volume Mesh tool in STAR-CCM+. A polyhedral mesher was used for this model, with prism layers near the walls.

A prism layer mesh model generates orthogonal prismatic cells around core volume mesh near the walls, surfaces, and boundaries. Prism layers, usually defined by their thickness and number of layers, allow solvers to resolve flows more accurately in the near-wall region.

The goal was to achieve a computationally light yet accurate model. Since the coupling process involves multiple iterations of the two simulations on TAITherm and STAR-CCM+, keeping the models light and the run times low was vital. These models were compared to a pre-tested calibrated model on STAR-CCM+. The mesh that was eventually used has about 80 million fluid cells.

As per TAITherm cabin thermal modelling guidelines [1], an attempt was made to change the prism layer thickness near the walls to achieve a y^+ value between 50 and 100. However, after repeated attempts, it was found that it was not possible to get a y^+ value between 50 and 100. Hence, the approach was changed to use the Specified y^+ Heat Transfer Coefficient instead. The Specified y^+ HTC is an option in STAR-CCM+ that allows one to evaluate the HTC at a user-specified y^+. This option allowed us to mesh the volume for better accuracy without considering the y^+ of near-wall cells. Once the mesh was generated and the simulation was complete, the HTCs were extracted from a y^+ of 100, as per the recommendation from STAR-CCM+. Other documents from STAR-CCM+ and TAITherm suggest using Specified y^+ HTC values below 30 and 10, respectively. However, the effect of using these values on the co-simulation was not tested as it was considered outside the thesis's scope.

3.1.2 Physics and Solver

In this chapter, we discuss the physics models and solvers used in STAR-CCM+ to simulate the flow in the cabin. The same physics model was used for all the simulations during this thesis. The physics models and solver settings were based on a previous study on the same bus.[7]

Physics

As discussed earlier in the Theory chapter, the K-Epsilon model was used to solve the turbulence in the simulation. This model was recommended in the previous study and is widely accepted in the industry. Since the velocities in the cabin are not very high, the flow is mainly defined by natural convection. The two-layer model has been converted from shear-driven to buoyancy-driven for natural convection. Similarly, based on another study on the same bus, the equation of state was selected as an ideal gas. This setting helps better solve the varying density rising due to the vertical temperature gradients.

Solver

This simulation uses a Coupled Flow solver that solves the continuity and momentum equations together as a vector of equations. It uses a Pseudo-Time-Marching approach, which includes a pseudo-transient term instead of the physical time derivative. The Coupled Flow solver gives a robust solution which is required for a robust coupling with TAITherm.[9]

3.1.3 Boundary Conditions

In this section, we have discussed how the boundary conditions have been modelled. The boundary conditions were applied for all the HVAC components to imitate the real-world conditions closely, using simulated physics instead. The boundary conditions have been modelled based on a previous study on the same bus model. The changes in these boundary conditions were only made to simulate different operating conditions and have otherwise remained unchanged. [7]

Roof Top Air Conditioning Unit

The rooftop air conditioning unit removes heat from the bus using an evaporator. It recirculates the cooled air in the bus using blowers. When the bus needs to be heated, the unit uses a heat pump to heat the air entering the cabin. A single-stream heat exchanger has been used to model the evaporator. When the unit is in cooling mode, heat is removed from the air, and when the cabin needs to be heated, heat is added to the cold air. This modelling option eliminates the need to model the evaporator and heat exchanger separately. This evaporator is modelled as a porous region to simulate the behaviour of the fins and thin tubes that the air passes through in the evaporator. The porous region replicates the pressure drop observed in the evaporator.
The air leaving the evaporator passes through 6 blowers fans placed evenly on either side of the roof unit. The blower fans are modelled as rectangular blocks, with the help of blower performance curves. They were treated as different regions with their inlets and outlets. The blocks perform as fans and work by generating a specific volume flow for the pressure at the inlet interface.

Defroster

The defroster in the bus was modelled to simulate the effect of a heat exchanger, evaporator, air filter and blower in a similar way as was done for the roof unit. Air enters the defroster naturally, passes through an evaporator and then a blower fan, which pushes the air into an air filter. The air enters the heat exchanger through the air filter and then is sent to the cabin. The pressure drop across the air filter, evaporator and heat exchanger is simulated by modelling these as porous media. The blower fans in the defroster are modelled like the fans in the roof unit. The blower performance curves have been received from the manufacturer and are used to get the volume flow from the fans.

Convectors and Heaters

The convectors and heaters are modelled as separate regions and wrapped and meshed as different regions. These are modelled as blocks, with inlet and outlet interfaces at the bottom and top of the regions. The heat rate of the convectors are defined as a product of the heat rate per meter and the length of the convector. The heaters are the same as the convectors but have a fan to use forced convection. The fans in these are modelled similarly to the roof unit using a fan curve provided by the manufacturer.

3.2 TAITherm Methodology

3.2.1 Geometry

In the previous thesis work [7], the whole bus geometry was divided into three ANSA files. The three ANSA files were taken and merged into a single ANSA file so that different parts in the ANSA files could be grouped. To properly implement TAITherm boundary conditions like the number of layers, materials used in different layers, air gaps, surface condition for radiation and initial temperatures, part IDs (PIDs) need to be created.

So, the workflow involved taking the merged file and giving PIDs to different parts by selecting and hiding the parts that need not be given PIDs. A major part of our thesis involved this pre-processing step since the whole bus geometry must be given PIDs. It involved much manual work that could not be automated as each part and, in many cases, surfaces must be examined individually. To give PIDs, the "Not" function, which hides a part/surface/PID, is used along with the "Set PID" options in the ANSA, which is used for giving PIDs to different parts.

From a previous thesis [8], material data for different parts of the bus chassis were obtained; this data included the number of layers each part had, the materials present in each layer, air gap thicknesses and surface area. Since there were 92 parts on the floor, 19 parts in the Front area, 7 parts in the roof area, 5 parts in the rear area, 47 parts in the left-hand side wall and 33 parts in the right-hand side area, it was decided to group the parts according to their similarity in material properties. Accordingly, the materials were grouped into 22 floor parts, 4 front area parts, 8 roof parts (since an extra part is added to the roof to make the model more accurate), 5 parts in the Rear, 17 parts on the left-hand side and 10 parts in the right-hand side. Since all the parts are similar but not identical, the material properties of the part having the highest surface area are considered the material property of the whole group of parts in a particular grouping. The original floor 3.5 is

compared with the floor after giving PIDs 3.6. Similarly, other parts were given PIDs. The PIDs given are shown for different walls of the bus.

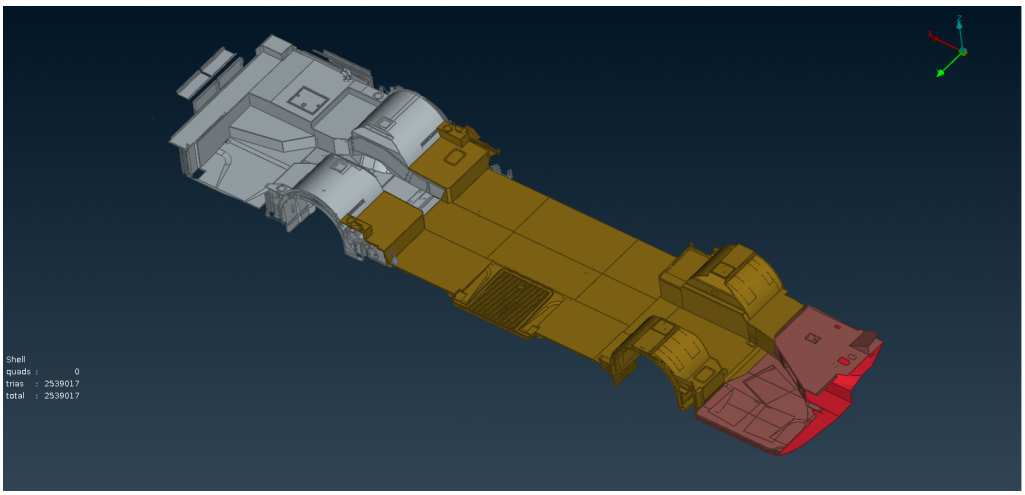

Figure 3.5: Original floor

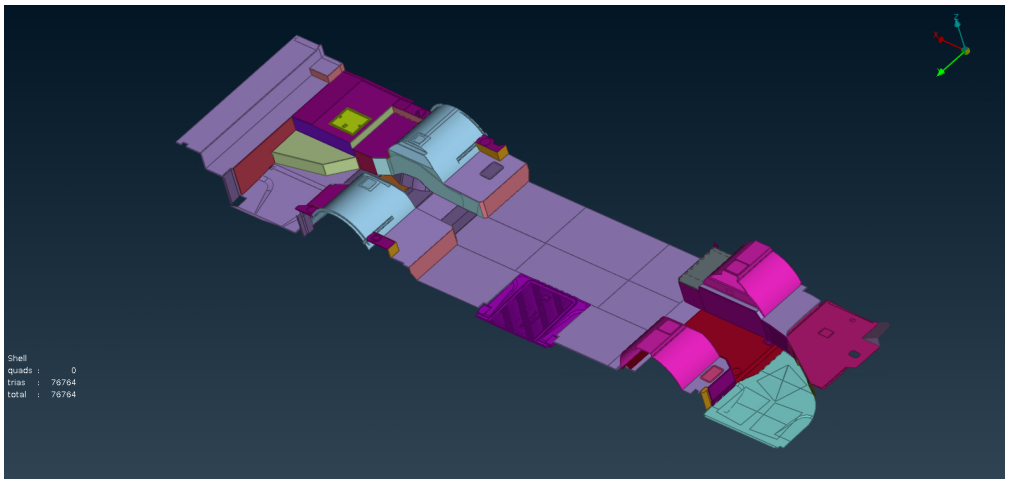

Figure 3.6: Modified floor

Similarly, other parts were given PIDs. The PIDs given are shown for different walls of the bus.
The resulting ANSA with the newly created PIDs is then exported to STAR-CCM+ using the .nas file format.

3.2.2 Mesh

The ANSA file with the newly created PIDs is exported to STAR-CCM+ to create a shell mesh for TAITherm. In STAR-CCM+, the surface wrapping and surface remesh process are carried out. After carrying out the surface remesh with the newly created surface wrap, only the surface mesh is exported without the internal water-tight volume; this is done by exporting the file in .nas file format, which only stores the surface mesh when exporting from a wrapped surface.

Surface Wrapper

An internal wrap is utilised here as the CFD data will be imported into the interior surface.

The same default and the custom controls used in the CFD model are used for creating the TAITherm wrap; this was done to keep the shape of the interior nearly identical to the CFD model. For this reason, the original

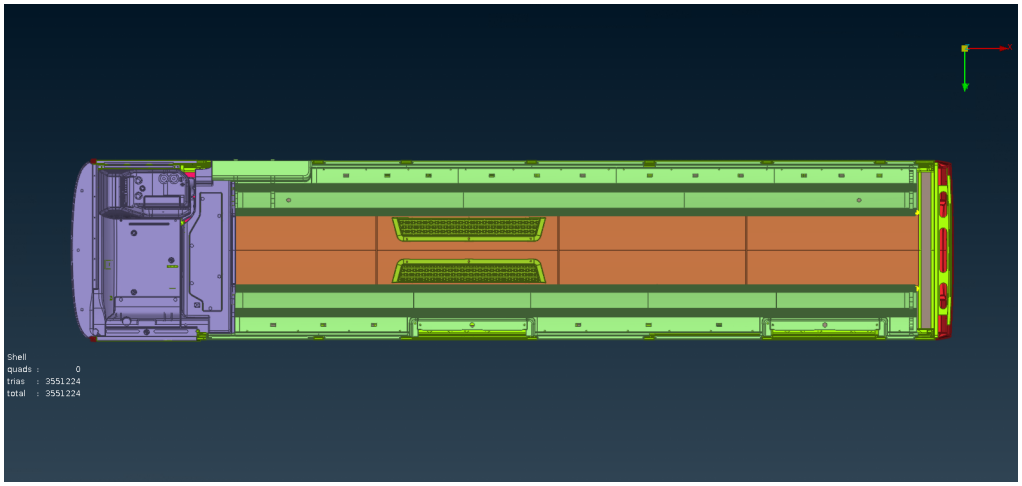

Figure 3.7: Modified roof

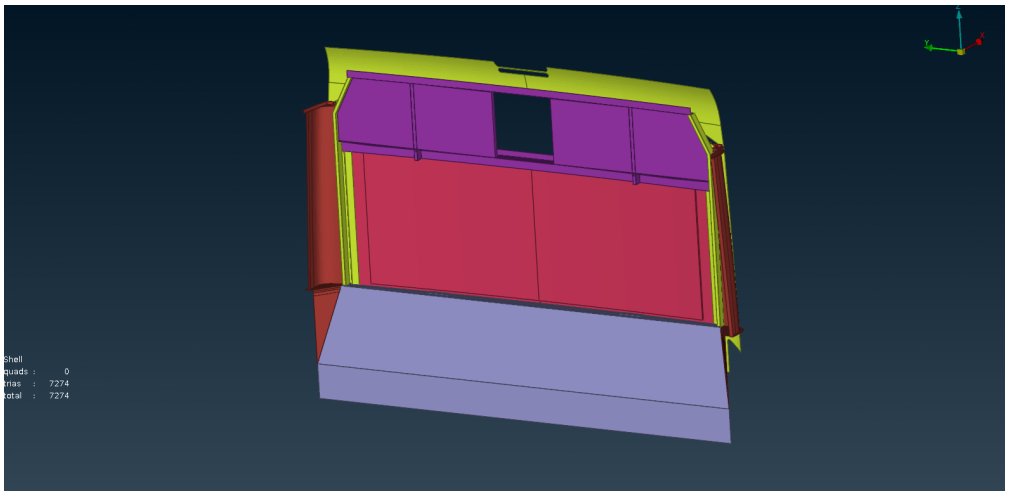

Figure 3.8: Modified rear

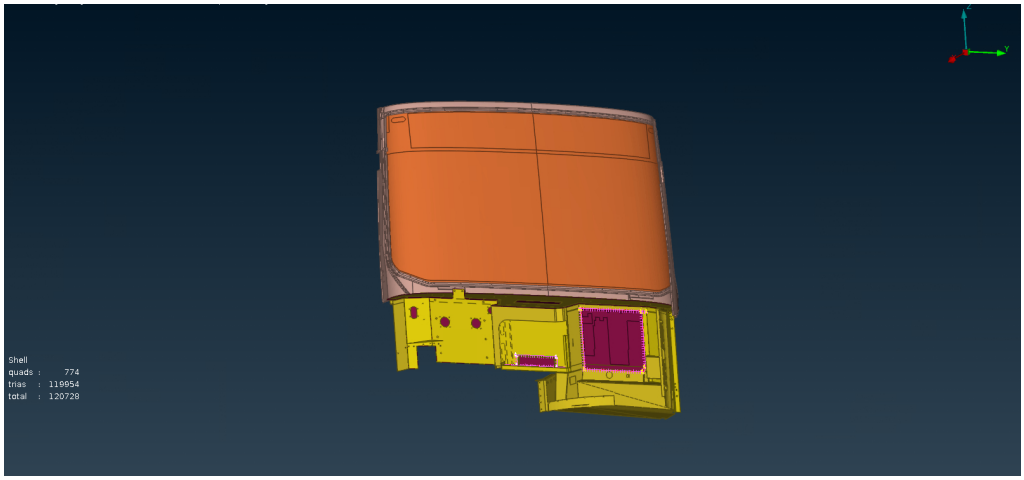

Figure 3.9: Modified front

Figure 3.10: Modified left-hand wall

Figure 3.11: Modified right-hand wall

parts from which the TAITherm parts were split were found, and the settings used by these parts for the CFD model were given to the TAITherm parts.

The normal orientation of the different parts of the geometry imported will not be uniform; the surface wrapper will fix this problem. After the geometry is wrapped, all the mesh parts will have normals pointing in the same front/back direction. Having a mesh with a uniform direction of normals is essential for TAITherm as having different normal directions will cause errors and increase the complexity of setting up the TAITherm.

Surface remesh

The coarsened CFD mesh obtained when exported to TAITherm led to problems with usability and crashes since the mesh had nearly 15 million elements. The CFD mesh used triangular mesh elements on the surface. STAR-CCM+ uses these mesh elements to create the volume mesh elements. In the case of TAITherm, quad-dominant meshes give better results since the faces are normal to each other in a quad-dominant mesh. So, the current mesh meshed using triangular elements was taken and converted to quadrilateral mesh.

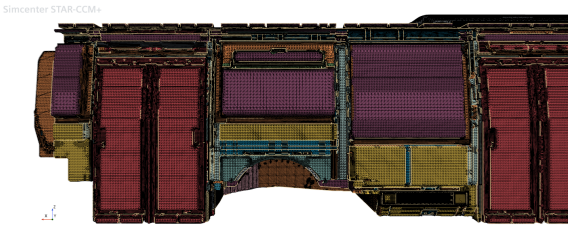

Figure 3.12: Surface wrapper

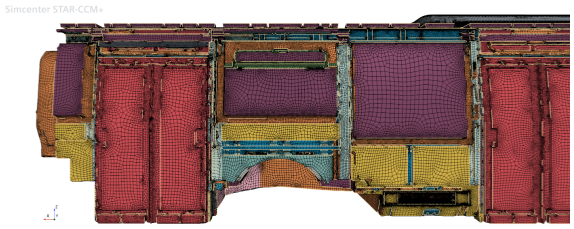

Figure 3.13: Remeshed surface

The obtained quadrilateral mesh is further coarsened while keeping the mesh at an acceptable quality. Proximity refinement was not performed like in the CFD mesh, as it only applies when creating volume meshes. Table 3.3 gives the trial to coarsen the mesh.

Number of elements	Base size(mm)	Target surface size (%)	Minimum surface size (%)	SGR
15044862	70	40	15	Default
7778577	105	40	15	Default
9325342	70	80	15	Default
7485494	70	80	15	Fast

Table 3.3: Automatic mesh coarsening

The final settings were used for automatic surface remesher, and the mesh obtained was below 8 million elements, so it worked without any usability issues and crashes in TAITherm GUI.

A comparison of meshed surfaces after and before the coarsening process is given below:

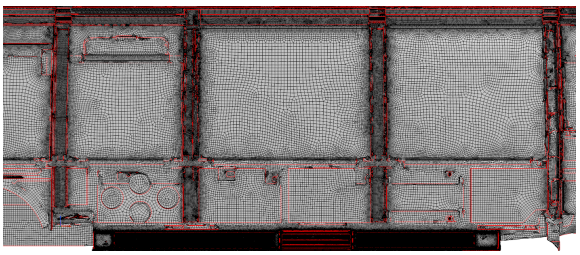

Figure 3.14: Remeshed surface

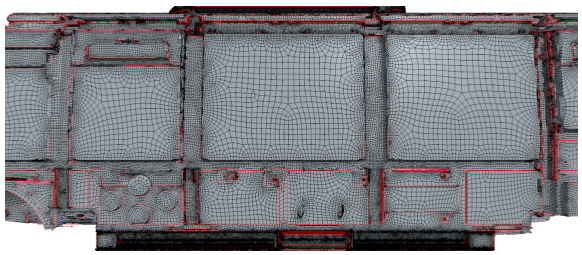

Figure 3.15: Remeshed surface coarsened

3.2.3 TAITherm setup

TAITherm material assignment and surface condition selection

The material data from the previous thesis [8] is used for all the PIDs that were grouped as explained in 3.2.1. For the surface conditions of the exposed parts and the air gap, the properties available in TAITherm that represent similar or the same material as the material property of the exposed layer are utilised. The initial temperature of all the parts is set to 15 degrees, the same as the initial static temperature in the CFD model.

External convection

The TAITherm library convection is not used for modelling the outside convection to reduce complexity. TAITherm library convection uses textbook convection correlations like the flow over a flat plate to calculate the heat transfer coefficient of air in contact with the surface. It requires input regarding the different lengths of the parts and the fluid properties [11]

Instead, the outside convection is modelled by giving the h and Tfluid as input. Since the outside air is still in the case of natural convection, according to the article [6], the h value of air can be between 2.5-25 $W/m^2.K$. Moreover, according to the TAITherm support site [5], a value of 5 or 10 $W/m^2.K$ is suitable for external natural convection. So, based on these two articles, the h value of still air which will come into contact with the outer surface of the bus is taken as 10 $W/m^2.K$. For the cases considered in this thesis, the temperature of outside air is taken as -5 ° C

Interior convection and CFD mapping

Using the STAR-CCM+ model, 3D CFD data is obtained. From the CFD model, the heat transfer coefficient and specific reference temperatures are obtained from a specific y+ value of 100 for the interior fluid part of the bus body; the reasoning for this specific value is explained in 3.1.1.

3.2.4 Solver settings

The multi-grid solver should be preferred whenever possible unless files for legacy versions of TAITherm need to be run [5]. Multi-grid is much faster than partial-direct and requires only a few iterations to converge compared to partial-direct; the solver uses grid refinement to correct errors that occur in places with coarser grids. The solver was set up based upon recommendations by ThermoAnalytics [5] to maximize stability. The recommended solver settings which were used in the thesis are described below:

- Inner Residual Convergence Criteria: Inner iterations are carried out to solve the linear part of the problem. The recommended option to improve efficiency is using the default "Scaled" with a value of 0.1. With this, if the residual becomes 1/10 of the original residual, the inner iteration is said to be converged.

- Maximum # inner iterations: Default value of 15 provides good performance as per support article from [5], and in case stability need to be further increased, this value should be made higher. 15 is used in this thesis.

- Relaxation: Default value is used, which resulted in good convergence. Reducing this value will positively avoid a diverging solution but will make the solver slower [5]. If the temperatures overshoot the solution, relaxation needs to be reduced. It was set to the default of 1.

- Matrix update frequency: Controls the number of times the solver preconditioner is run; if it is run more often, the stability will increase, but it will have a performance penalty [5]. In the run cases, setting this option to medium worked well.

- Number of radiation sweeps: Sets the number of inner iteration radiation sweeps; increasing will increase stability [5]. The solution converged well with this parameter set to 2.

3.2.5 View factor calculation

During the initial trial phases, it was found that using the current computational resources available for TAITherm, the calculation of the view factor with the "Calculate from Element Subdivisions and Averages for Patch" method was not feasible for the 8 million elements in the mesh as the view factors here are calculated for each element and patches. So, "Calculate from Patch Centroid Only" method is considered where the elements were grouped into patches to speed up the view factor calculation. The view factor here is calculated from the element centroid closest to the whole patch's centroid. In this method, the view factor calculation takes place much faster but has less accuracy.

After a quick study with simple geometry, the number of rays is kept at the default value of 1153. Increasing the number of rays had a negligible effect on the net radiation heat transfer; this was tested using some selected elements on the simple geometry. On the other hand, increasing the number of rays considerably increased the computational resource and the time required to get a solution.

Patch settings

The view factor calculation was limited to 25 elements per patch, with a maximum normal deviation of 20 degrees. The view factors were tested for 50 and 100, which executed faster. However, to increase the accuracy of the view factor calculation, it was pushed to 25 elements per patch, which took around 48 hours to calculate the view factors.

The view factor calculation needs to be run only once, and the same can be used for different material assignments and number of layers as long as there are [5]:

- No geometry changes
- No view factor settings change
- No environment changes

3.2.6 Thermal linking

The surface wrapper could not include a sizable amount of parts. These parts are crucial for conduction and radiation in TAITherm. These parts should ideally be included through the thermal linking feature of TAITherm, which allows heat transfer between the parts that are not in contact. There are two types of thermal linking: face-face thermal linking and generic thermal linking. Face-face thermal linking must be used here because only conduction needs to be considered for the extra parts. Since thermal linking involved much manual checking, which increased the probability of human error and consumed much time with the limited computational resources, a decision was made to avoid using thermal linking for this thesis.

Removing air gaps greater than 12.7mm

When the TAITherm file was being set up, it was noticed that parts had air gaps of more than 12.7mm. If the air gaps are larger than 12.7mm, it falls outside the validation range of the empirical formula used by TAITherm 2.2.6. To avoid that, the air gaps were initially split and embedded into different surfaces instead of having one large air gap. However, with this approach, the air gap will introduce more radiation between the gaps that should not exist in the first place. So, the accuracy error due to air gaps being larger than 12.7mm was accepted for some parts. For parts having substantial differences in comparison with the recommended range, the air gaps were considered part of the outer body, which was not considered in the study.
Before removing the larger air gaps, another method was considered to include the air gaps by using a hollow cylinder type. This idea is not carried forward as, in a part, a single layer alone cannot be of cylindrical conduction type, and cylindrical conduction type has its drawbacks as discussed in the section 2.5.

Assumptions for parts that do not have material properties

To reduce the weight of the entire bus chassis, it is a standard practice in the industry to use aluminium for the majority of the parts, so for parts of the bus which lack material properties, data like the material, number of layers and air gaps present the parts is assumed to be made up of aluminium with a thickness of 3mm. Future work can be focused on giving the exact material data to the assumed parts to improve the reliability of the results.

3.2.7 Effect of mass on transient simulation and checking the mass

When carrying out transient simulations, the left-hand side of Eq.2.13 will not be zero; this will affect results obtained as explained in section 2.2.4. So, checking the mass of the total bus body before running the simulation is crucial. The mass was checked using a Python script obtained from [5] that calculated the mass of each part and then added them together. The final file used in the thesis had a reasonable mass when not considering the outer body and also heavy equipment like batteries.

3.2.8 Tolerance selection

The tolerance slope is the ° C change per iteration. It is fixed to 0.001 for steady-state analysis; the value was obtained after observing the temperature change per iteration after convergence fluctuating with a difference of 0.001 ° C. For the transient analysis, this criteria is slightly relaxed to 0.01 ° C, to allow for reduced solving times.

3.3 Coupling Methodology

A pseudo-transient coupling methodology was adopted, with CFD running only in a steady state. When a transient-transient coupling is carried out, a very small time step needs to be given to the CFD model compared to the thermal model to resolve the fluid flow accurately. This approach is extremely slower as the thermal solver has to wait for the fluid solver to catch up to the real time before proceeding to the next step. To avoid such a problem, it is recommended to use a pesudo-transient model, where the CFD is solved using steady state simulation, and the values are then imported to a thermal solver, which runs in transient. Here, the thermal solver can take larger time steps to get a faster solution without waiting for results from CFD, as the CFD results are already available at the keys points.

Figure 3.16 showcases the overview of the pseudo-transient coupling methodology followed.
The boxes in Figure 3.16 are coloured to indicate different processes. Blue is used for CFD simulations; Yellow is used for TAITherm simulations; the Green arrow indicates a coupling between the two blocks, and the blue arrow indicates that the information transfers without coupling. It can be observed that there is a steady state coupling happening between 1^{st} and 2^{nd} block. The iterations between 1 and 2 are carried out till convergence of average surface temperatures in TAITherm and volume averaged field mean temperature are obtained; more details about the procedure to check for convergence are given in section 3.3.

The next block, 3, is then run, which takes the results from block 2 as initial conditions. Block 3 uses h and Tfluid values from 1 at 0 mins and h and Tfluid values at 5 mins as boundary conditions. The coupling between blocks 3 and 4 is carried out by only changing the h and Tfluid values at 5 minutes till the two convergence criteria mentioned before are satisfied. For this coupling process between 3 and 4, another criterion should be checked: the percentage deviation of HTCs, refer 3.3. When this criterion is satisfied, the coupling is said to be converged and then proceeded to the next block.

A feature called transient restart is used for block 5. This feature allows TAITherm to start from the end of block 3 with added time step used in block 5. In block 5, only the CFD results at time 15mins is imported and mapped into the TAITherm file. Now, the coupling between blocks 5 and 6 is carried out till all three convergence criteria are satisfied.

For the case run in the thesis, all the HVAC components are allowed to run at 100% at the start, i.e., 0 mins, and then all the HVAC components are turned off. So, the CFD - steady state results at 5 mins is the whole

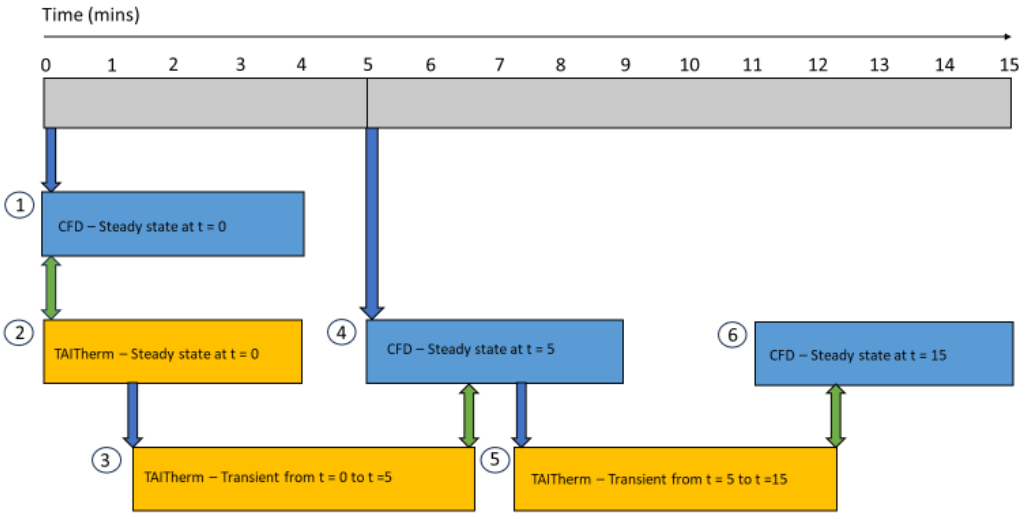

Figure 3.16: Overview of the pseudo-transient coupling process

bus body just exposed to the environment for 5 mins after all the HVAC components are turned off. Similarly, CFD - steady state results indicate that the bus body is exposed to the environment without HVAC for 15 mins.

When transitioning from block 4 to block 5, it is noted that CFD - steady state results at block 4 is the same as the CFD - steady state results at block 6 initially since the CFD is not run in transient. Since block 5 is initialised with transient restart, it will have the temperature values after the bus is exposed to the environment for 5 mins; the results after running block 5 will then be transferred to block 6. Now, the solution after carrying out block 6 will be different from the solution of block 4.

Export procedure from STAR-CCM+

To export the steady state results from the CFD model in STAR-CCM+, a XYZ table is created with the parameters shown in Figure 3.17.
The parameters mentioned above are exported for only the convective wall boundaries of the fluid region, as shown in Figure 3.18.

Import procedure in TAITherm

The data exported from STAR-CCM+ is then imported into TAITherm using a .csv file. The imported values are only applied to the back side of the TAITherm mesh, as the back side faces the bus's interior. The same is shown via an image in 3.19.
When mapping from TAITherm to STAR-CCM+, care should be taken so that the face that is in contact with the fluid in STAR-CCM+ is mapped onto the same front/back side of the TAITherm mesh [5]. CFD normal convection is kept as "Into Wall" see Figure 3.20 as the CFD data is inward or in the direction of the back face [11].

Export procedure from TAITherm

After TAITherm completes the thermal simulation, the temperature results from the back or the wall faces, which are in contact with the fluid, are extracted using vertex-based results. Geometry is exported with a meter as a unit. Refer to Figure 3.21.

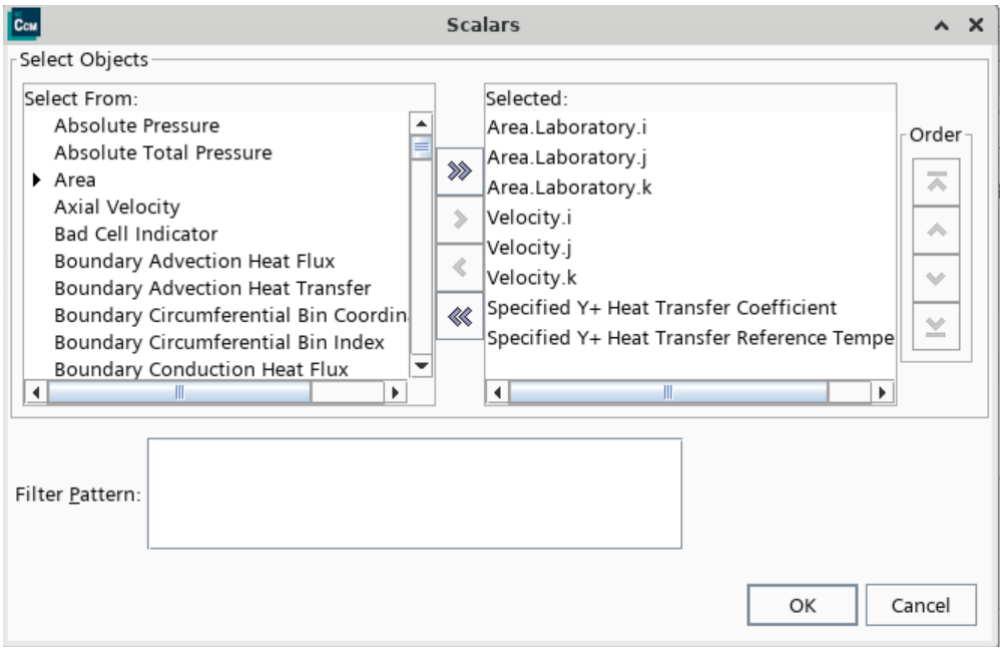

Figure 3.17: Scalars exported

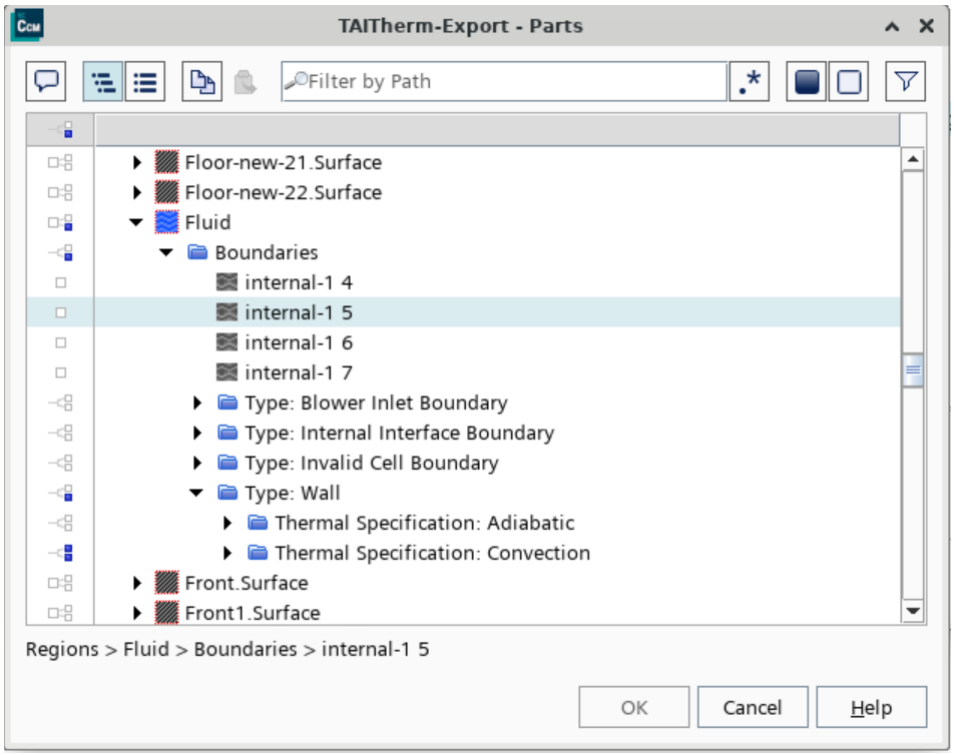

Figure 3.18: Parts of scalar export

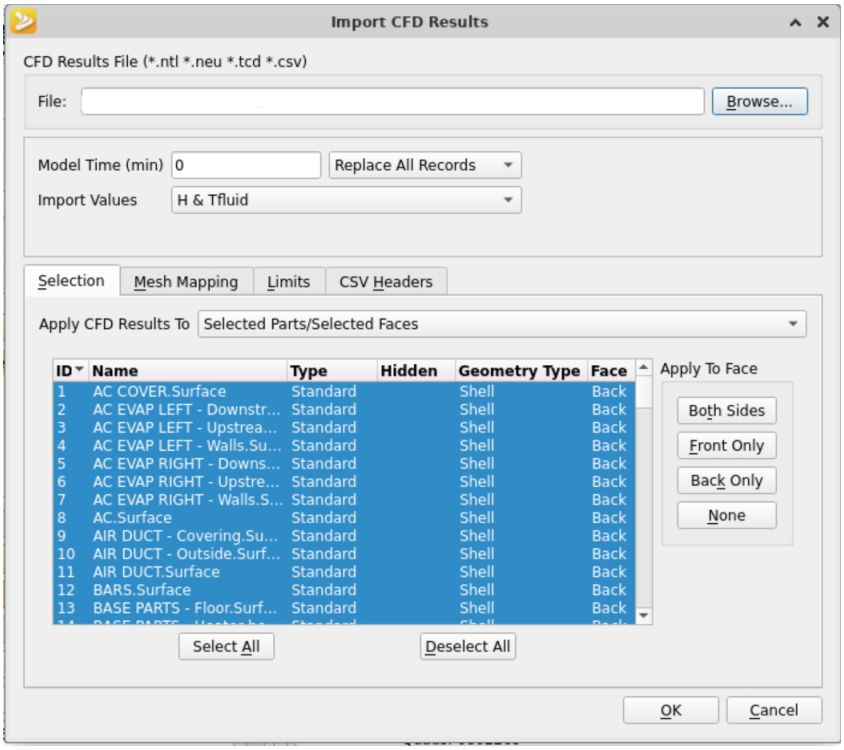

Figure 3.19: Importing into TAITherm - Selction

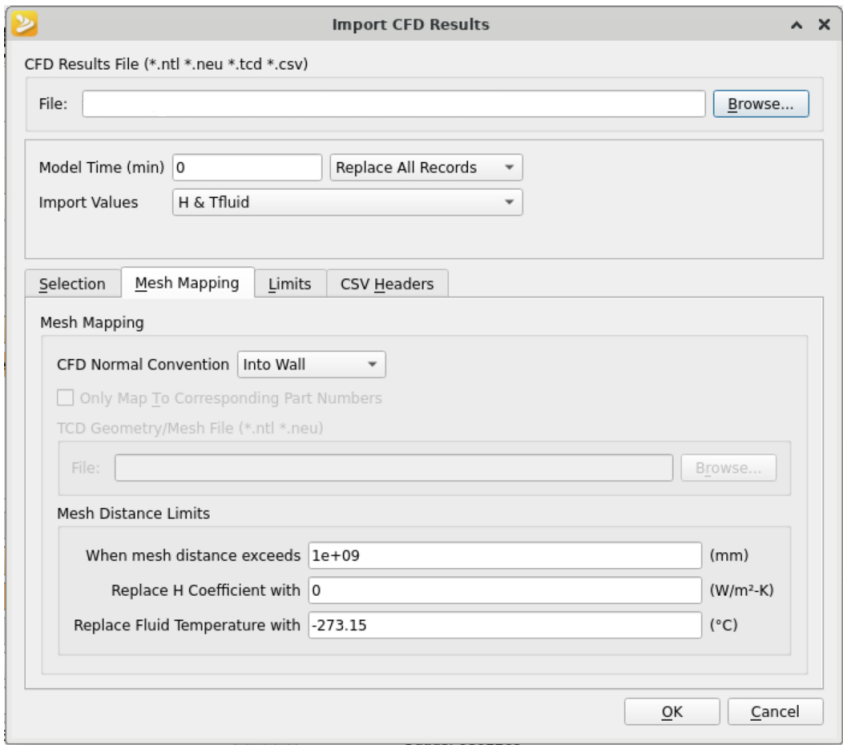

Figure 3.20: Importing into TAITherm - Mesh mapping settings

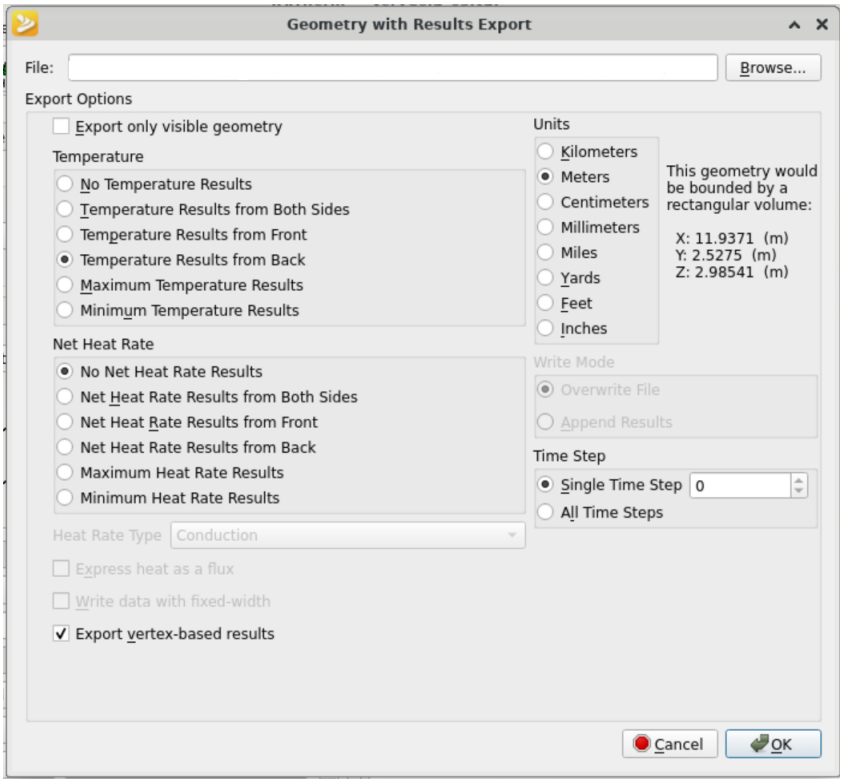

Figure 3.21: Exporting from TAITherm

Import procedure into STAR-CCM+

The step-by-step procedure to import TAITherm results into STAR-CCM+ for the first time is shown below:

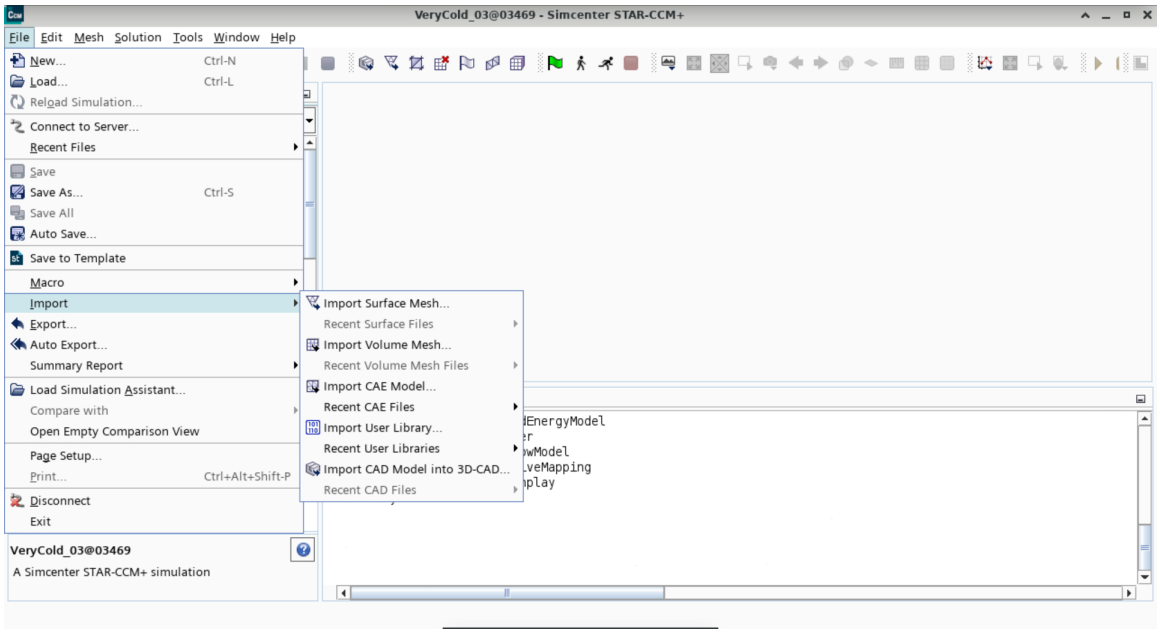

Figure 3.22: Importing into STAR-CCM+ - Import CAE

As shown in 3.25, units of temperature should be K. When the results are exported from TAITherm using meters as units, TAITherm stores the temperature data in K.

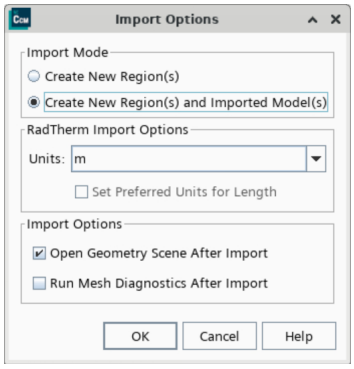

Figure 3.23: Importing into STAR-CCM+ - Import CAE2

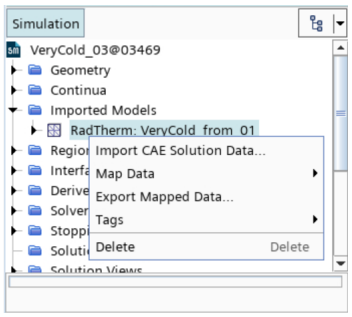

Figure 3.24: Importing into STAR-CCM+ - Import CAE solution Data

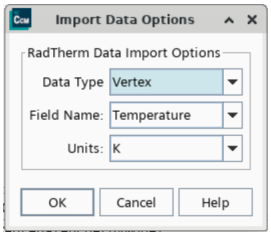

Figure 3.25: Importing into STAR-CCM+ - Import CAE solution Data settings

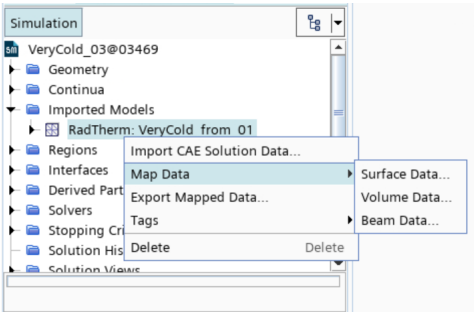

Figure 3.26: Importing into STAR-CCM+ - Map data

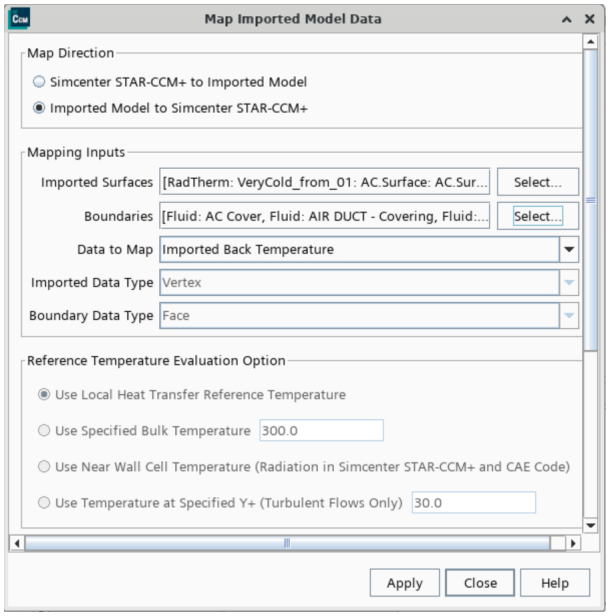

Figure 3.27: Importing into STAR-CCM+ - Map data settings

After mapping the results, a field function called "MappedImportedBackTemperature" will be created; this should be used as static temperature for convective walls in the fluid region.

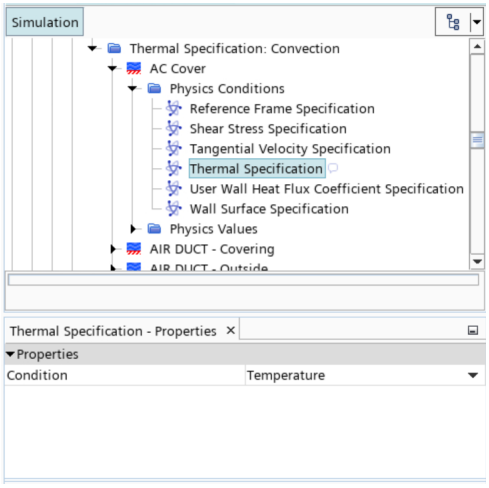

Figure 3.28: Importing into STAR-CCM+ - Changing thermal boundary conditions at walls

Procedure to check coupling convergence

As mentioned earlier in section 3.3, for the coupling between CFD-steady state and TAITherm steady, two convergence criteria are looked at, namely, surface average temperatures (an average of all nodes in a part should be taken) and volume averaged field mean temperature. For the coupling between CFD-state and TAITherm transient simulations, an additional criteria of HTC is taken into account.

Since there are more than 100 parts in TAITherm, only six parts close to the sources, i.e., AC unit, heat blower, convector and defroster, are considered for measuring the surface average temperatures. These parts were selected as they will have the maximum temperature change.

For checking the HTC convergence, initially, six parts were taken from the CFD model and their local HTC

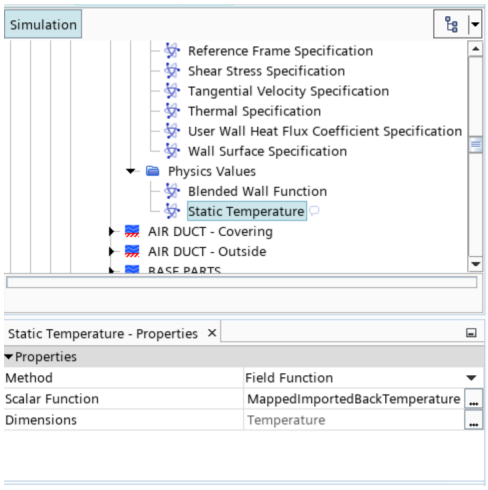

Figure 3.29: Importing into STAR-CCM+ - Field function for boundary condition

change were studied. Local HTC is selected instead of the specified y+ HTC value as the specified y+ values might change with the solution, unlike local HTC values making it easier to compare the HTC change across the coupling iterations. The method used to compare the HTCs involved creating a table in STAR-CCM+ to export the values and processing the data in Excel manually for comparison; this process created a bottleneck and consumed much time. So, from the six parts studied, only three with the most HTC percentage change are selected. The percentage change of HTC every coupling iteration is compared with the previous coupling iteration. The criteria are satisfied if the percentage change from the previous iteration is low.

The convergence plots and data are provided in the results section 4 for the case considered in the thesis.

4 Results

4.1 CFD mesh coarsening results

As discussed earlier, the CFD mesh had to be coarsened from the original mesh to reduce the run times. This was done to ensure that the simulation was viable while coupling multiple times for the co-simulation. From the multiple cases that were tested, below is the plot comparing the normalised values of the Mean temperatures in the bus for the whole region. The maximum deviation from the Original Mesh to the Final mesh was observed to be less than 1 degree Celsius. Although the other test cases look closer in results to the original mesh, their run times did not significantly improve. The total simulation time for the Final mesh case was slightly above 4 hours, drastically improving from the 8 and 9 hours required for the other test cases. Due to this, we decided to go with that particular mesh, with about 80 million fluid cells, as the final mesh.

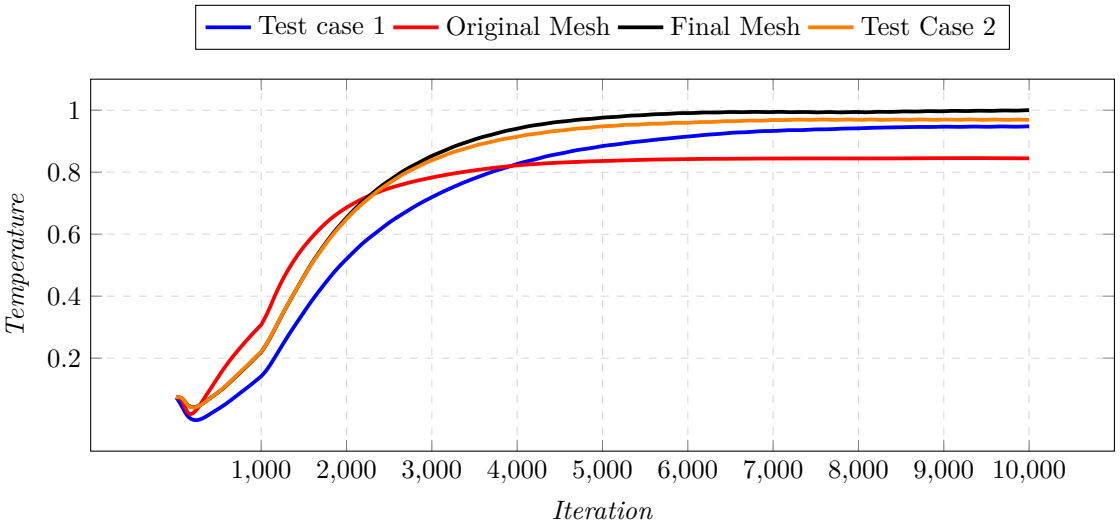

Figure 4.1: Comparison of Field Mean Temperature

4.2 Coupling convergence criteria

As discussed in section 3.3, field mean temperature and average surface temperature are used as convergence criteria for steady coupling, i.e., coupling between blocks 1 and 2 in Fig. 3.16. Additionally, HTC change is looked at for transient couplings, i.e., coupling between blocks 3 and 4, and coupling between 5 and 6 refer Fig. 3.16.

4.2.1 Average surface temperature

Figures 4.2, 4.3 and 4.4 indicate normalized temperatures over coupling iterations for different parts chosen from the rear, front, side walls and roof. The averaged node surface temperature taken for the case used in the thesis will usually converge in the second or third iteration, but to have a more explicit representation of the convergence, the fourth iteration is carried out at all stages. From Figures 4.2 and 4.3, one can see that the temperature does not change much after the second iteration. Figure 4.4 also shows convergence, but it cannot be shown accurately in the normalized plot as the values are very low. The temperature convergence indicates that the TAITherm side of the methodology has reached coupling convergence.

4.2.2 Field Mean Temperature

Similar to surface averaged temperature, the volume-averaged field mean temperature should be looked at to check the coupling convergence in the CFD model. Figures 4.5, 4.6, and 4.7 show the convergence of Field Mean

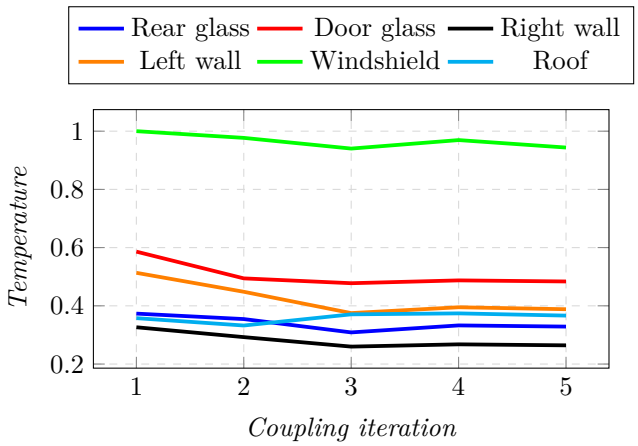

Figure 4.2: Surface average temperatures of 2 refer Fig. 3.16

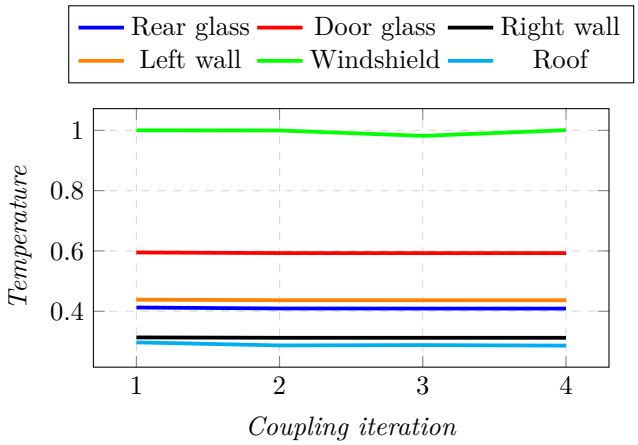

Figure 4.3: Surface average temperatures of 3 refer Fig. 3.16

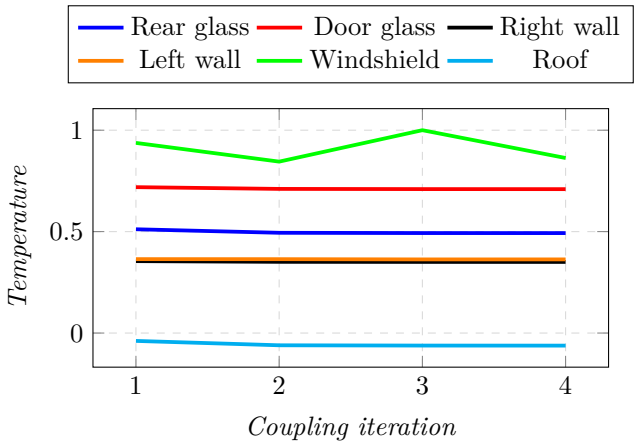

Figure 4.4: Surface average temperatures of 5 refer Fig. 3.16

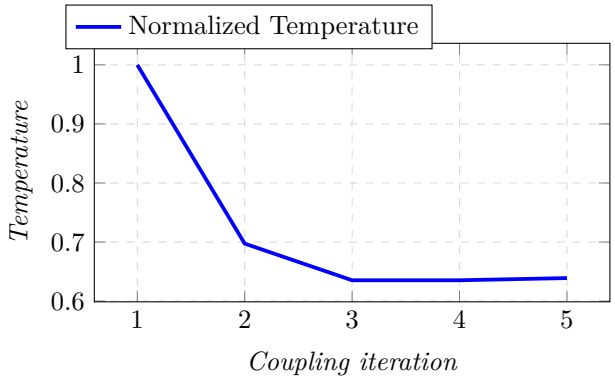

Figure 4.5: Field Mean Temperature for coupling between 1 and 2 refer Fig. 3.16

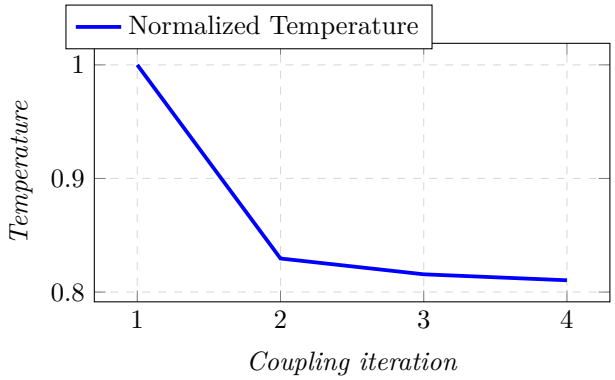

Figure 4.6: Field Mean Temperature for coupling between 3 and 4 refer Fig. 3.16

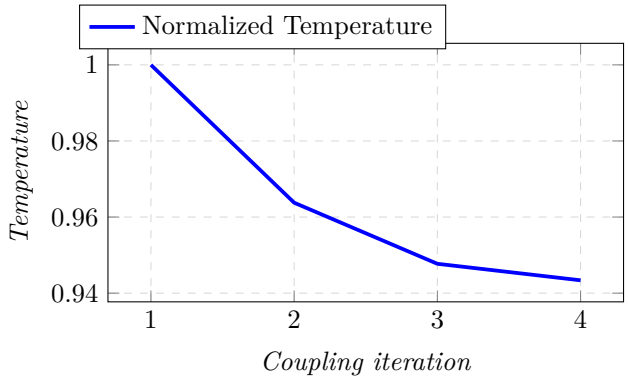

Figure 4.7: Field Mean Temperature for coupling between 5 and 6 refer Fig. 3.16

Temperatures. In Figure 4.7, the values of all the coupling iterations are very close, with around 0.1 to 0.2 degree variation, so the normalized graph does not correctly show the converging of Field Mean Temperature.

4.2.3 HTC

An additional checking criterion is imposed for the coupling of blocks 3 and 4 and coupling of blocks 5 and 6, as shown in Fig. 3.16. In these couplings, the percentage of HTC change is measured from the CFD model for all the near-wall cells in three selected parts. This measurement ensures that the TAITherm transient reaches the required HTC at the end of the transient simulation. The coupling in these cases is considered converged if the HTC percentage change between the iterations is meagre. From the Tables 4.1, 4.2, and 4.3, it can be seen that the maximum percentage change is around 2.4%, which is a very low percentage change. So, the coupling criteria are considered satisfied.

Time (mins.)	**Avg.% change from 1 to 2**	**Avg.% change from 2 to 3**	**Avg.% change from 3 to 4**
5	0.55	0.49	0.57
15	0.57	0.56	1.31

Table 4.1: HTC change comparison of part 1

Time (mins.)	**Avg.% change from 1 to 2**	**Avg.% change from 2 to 3**	**Avg.% change from 3 to 4**
5	0.77	0.90	1.01
15	1.41	1.29	1.09

Table 4.2: HTC change comparison of part 2

Time (mins.)	**Avg.% change from 1 to 2**	**Avg.% change from 2 to 3**	**Avg.% change from 3 to 4**
5	0.11	0.04	0.03
15	0.05	0.04	2.49

Table 4.3: HTC change comparison of part 3

4.3 TAITherm results

4.3.1 Comparison of parts at 0 minute and 15 minutes

After running the complete methodology using the pseudo-transient model for 15 minutes, the surface temperatures were analysed in TAITherm at the start, 5 minutes and 15 minutes after the start. The heat lost to the environment over time is visualized in the following images:

Bus body - Outside view

Figures 4.8, 4.9, and 4.10 show a heat source in the front of the bus. The heat source is nothing but the defroster. Five minutes after the defroster is switched off, the walls of the defroster cool down upon exposure to the cold weather outside the bus. Finally, 15 minutes after the defroster is switched off, the walls of the defroster have a temperature close to the front walls of the bus.

Windshield - Front view

From Figures 4.11, 4.12 and 4.13, one can notice that the windshield loses its heat from top to bottom; this is because the defroster located at the bottom of the windshield is responsible for heating up the windshield. When the defroster switches off, the region of the windshield close to the defroster walls remains hot as the heat retained by the defroster walls gets transferred to the windshield. At 15 mins, refer 4.13, all the heat available to the windshield gets dissipated.

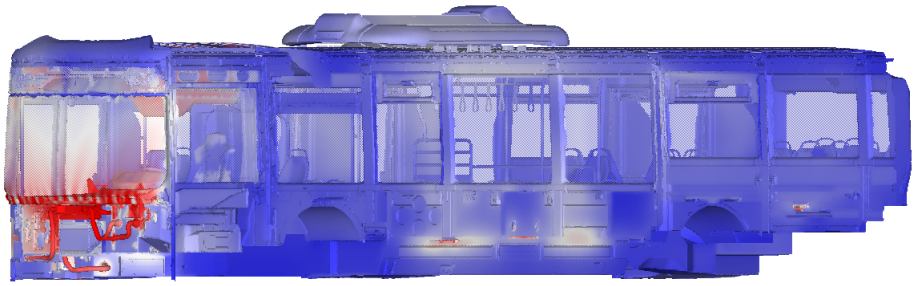

Figure 4.8: Temperature of bus body from outside at time = 0mins

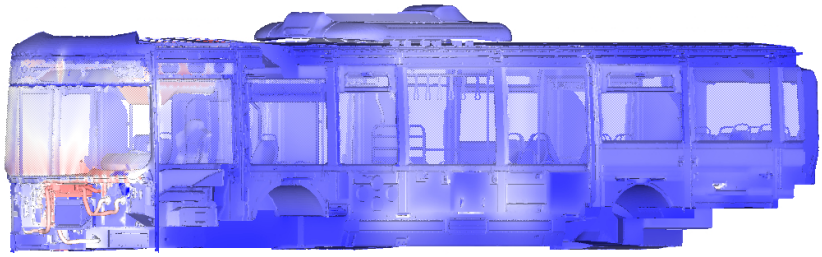

Figure 4.9: Temperature of bus body from outside at time = 5mins

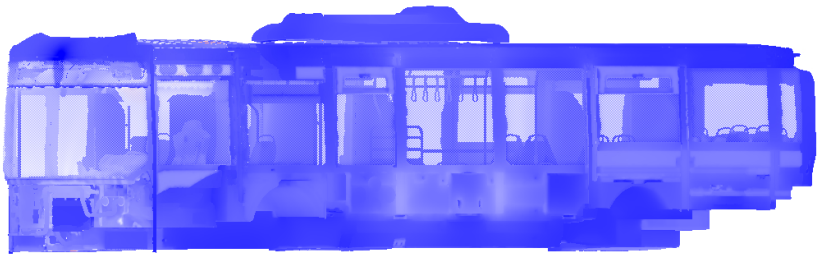

Figure 4.10: Temperature of bus body from outside at time = 15mins

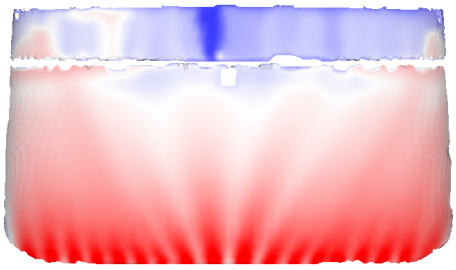

Figure 4.11: Temperature of windshield at time = 0mins

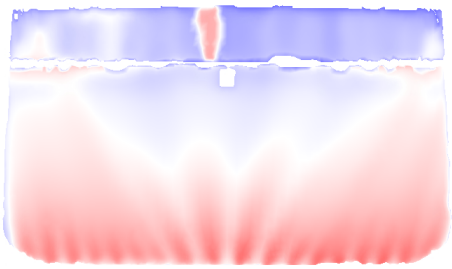

Figure 4.12: Temperature of windshield at time = 5mins

Figure 4.13: Temperature of windshield at time = 15mins

Left-hand wall - Side view

On the side walls, convectors and heat blowers are present, which heat these walls and the surrounding air temperature when the bus is run in a very cold environment. Figure 4.14 shows the presence of the heat source at the left-hand side wall, which, after getting turned off, gradually cools down the wall as shown in figures 4.15 and 4.16.

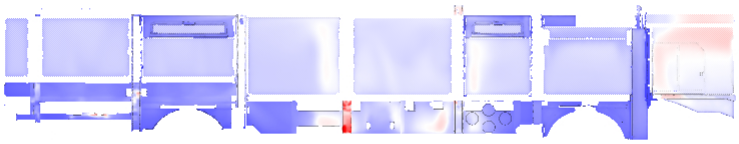

Figure 4.14: Temperature of left hand wall at time = 0mins

4.3.2 Heat loss from the interior of the bus

Since the CFD model is not run transient, the interior field mean temperature could be measured only at three-time instances, i.e., at t = 0 mins, t = 5 mins and t = 15 mins after switching off the HVAC systems. Figure 4.17 shows the interior FMT temperature measured. The temperature of the air inside drops as expected due to heat transfer from the interior to the outside cold environment.

4.3.3 Heat loss from different parts

The parts selected for checking convergence are close to the heat sources, which makes them ideal for testing heat losses from the bus interior to the environment. Figures 4.18 and 4.19 show the heat loss from the selected parts; the same value normalizes both Figures. The part selected from the Roof and the windshield have a

Figure 4.15: Temperature of left hand wall at time = 5mins

Figure 4.16: Temperature of left hand wall at time = 15mins

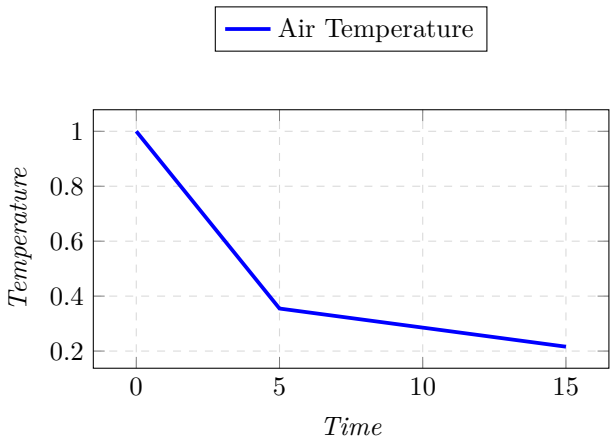

Figure 4.17: Interior temperature drop over time

faster heat loss rate than the other four parts shown in Figure 4.18. Upon investigation, both parts seemed to be single layers without adding insulating materials. So, adding an insulation or air gap can make these parts lose heat at a slower pace.

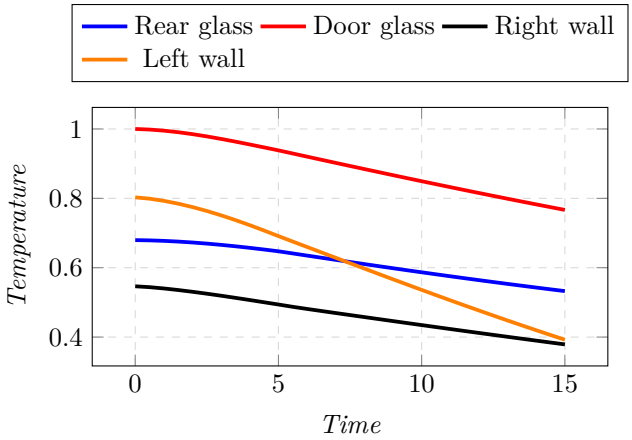

Figure 4.18: Parts with slow temperature drop

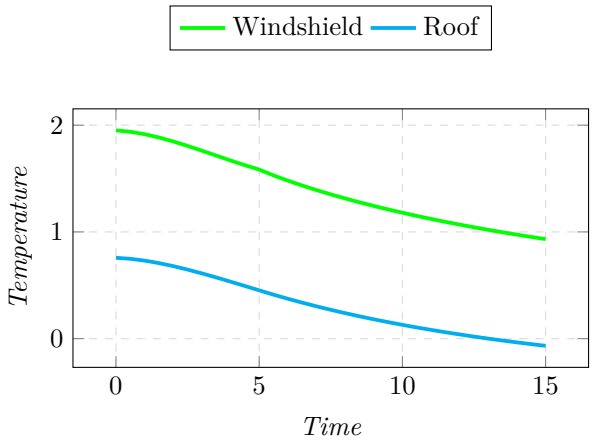

Figure 4.19: Parts with fast temperature drop

5 Conclusions

This study aimed to develop a method for a pseudo-transient co-simulation using STAR-CCM+ and TAITherm for the bus body. This chapter includes a summary of the most important outcomes from the thesis.

The mesh study leads to the following conclusions. The CFD mesh on STAR-CCM+ was essential to get right. The mesh had to be computationally light while maintaining high accuracy. It starts with careful execution of the surface wrapper. It was important to accurately capture all the geometry while staying moderate with the cell count. As discussed earlier, this could be done with the use of custom controls. The surface mesh acts as a base for the volume mesh, and getting this right goes a long way in reducing bad volume mesh, ultimately resulting in higher stability of the solver. On the TAITherm side, the main aim was to keep the mesh light. However, since the results from TAITherm get mapped onto the mesh in CFD, there was still a requirement to keep the cell count of CFD mesh within a reasonable range.

Since the Specified Y+ Heat Transfer Coefficient approach was used, the y+ values could be kept low in the CFD simulation, hence allowing the simulation to converge quickly. The y+ values were kept below 100 using prism layer cells near the surface. The y+ values can be influenced by keeping the cell size low near the wall boundaries. It was found that it was also important to use buoyancy-driven convection since most of the flow is dominated by slow-flowing regions, leading to most of the flow being driven by natural convection.

In the TAITherm, giving PIDs is a time-intensive activity. To save time, all the parts were grouped based on available material property data, reducing the total number of PIDs present. The same surface wrap settings from the CFD model were used to create the surface wrap for the TAITherm model to obtain the same bus interior shape. The obtained wrap is meshed with quad-dominant elements and coarsened further to make the mesh usable in TAITherm.

The TAITherm model was set up with materials properties, including the thickness, number of layers and air gap according to the available data. The surface conditions for these parts were selected to emulate the material of the exposed parts. External convection is included using h and Tfluid value of 10 $W/m^2.K$ and -5 $^\circ$ C, respectively. Interior convection is included using the h and Tfluid data obtained from CFD at a y+ value of 100. The solver settings recommended by TAITherm support were utilized for greater stability. For view factor settings, the highest possible refinement with patches considering the limitations on the computational resources was utilized. No parts were thermally linked, avoiding complexity in the case. The material properties of parts without material data are assumed to be aluminium. Major air gaps were not included and considered part of the outer body. The mass of the whole bus body was checked so that transient simulations were accurate.

The TAITherm and CFD models were then coupled and run for 15 mins after switching off the HVAC systems. The coupling methodology had three coupling points where the criteria for convergence were checked. At the end of 15 mins, the heat loss from different bus surfaces and the heat loss from the interior were visualised. The results indicated that the pseudo-transient coupling methodology established works as expected.

A further analysis was carried out to compare the heat losses from different parts over time to identify the part losing the most heat. The part was then analyzed to suggest changes or improvements. Similarly, if all the bus parts are looked at individually, and insulation is added to the parts losing the most heat, it would significantly reduce the total heat loss from the bus interior. Lowering the total heat loss will allow the HVAC systems to operate less frequently in cold weather conditions, reducing power consumption.

5.0.1 Future Work

- Due to lack of time, certain aspects of the thesis were left out and could be considered as part of a future study. Our first recommendation would be to validate the model with experimental test results. This would be able to provide more data to calibrate the model.
- The model could also be further developed by including the body's external parts in the simulation. This could be done using the thermal linking function in TAITherm and an external surface wrap in

STAR-CCM+. Doing so would allow the model to include many more variables than both of these software allow for, although increasing the complexity of the model vastly. A few such things that can be included on the TAITherm end for thermal modelling are solar loads and passenger loads. Setting up a CFD simulation for wind on the outer part of the body and including these in the simulation could help get better results and better understand the heat transfer through the bus body.

- Once the model is validated and calibrated, different materials can be tested and simulated on the TAITherm model to study their effect on the heat transfer through the bus body. This information can help the design in a way to reduce the losses in the system.
- Conduction rules can be studied to see how information from different layers of different parts communicates with each other, i.e., how conduction is carried out from one layer to another.
- Automating the whole coupling process could be carried out to save the time spent on manual coupling.

References

[1] *Cabin Thermal Modeling Best Practices Guide*. ThermoAnalytics, Inc., 2008.

[2] L. Davidson. *Fluid mechanics, turbulent flow and turbulence modeling*. Chalmers University of Technology, 2023. URL: https://www.tfd.chalmers.se/~lada/postscript_files/solids-and-fluids_turbulent-flow_turbulence-modelling.pdf.

[3] M. Ekh. *Mechanics of solids fluids – introduction to continuum mechanics.* Chalmers University of Technology, 2020. URL: https://www.tfd.chalmers.se/~lada/MoF/postscript/lecture_notes_continuum_mechanics_2020.pdf.

[4] E. E. Johansson and M. Skärby. Interior climate simulation of electric buses. *Master's thesis - Department of Mechanics and Maritime Sciences* (2019). DOI: https://hdl.handle.net/20.500.12380/257071.

[5] Knowledge base - TAITherm support (2023). DOI: https://support.thermoanalytics.com/hc/en-us.

[6] P. Kosky et al. *Chapter 12 - Mechanical Engineering*. Academic Press, 2013, pp. 259–281. DOI: https://doi.org/10.1016/B978-0-12-415891-7.00012-1.

[7] N. B. Ravindra. Unsteady Interior Climate Simulation of Electric Buses. *Master's thesis - Department of Mechanics and Maritime Sciences* (2020). DOI: https://hdl.handle.net/20.500.12380/301055.

[8] H. Sahraei. Interior Climate U-Value calculation and optimization for electric buses at Volvo buses. *Master's thesis - Department of Mechanics and Maritime Sciences* (2020). DOI: https://hdl.handle.net/20.500.12380/300921.

[9] *Simcenter STAR-CCM+ - User Guide*. Siemens, 2023. URL: https://support.sw.siemens.com/.

[10] *UN Sustainable Development Goals*. UN Department of Economic and Social Affairs, 2023. URL: https://sdgs.un.org/goals.

[11] *User Guide TAITherm Version 2022.2.1*. ThermoAnalytics, 2022.

DEPARTMENT OF MECHANICS AND MARITIME SCIENCES
CHALMERS UNIVERSITY OF TECHNOLOGY
Gothenburg, Sweden 2023
www.chalmers.se

CHALMERS
UNIVERSITY OF TECHNOLOGY